

**The Alzheimer disease-related presenilin-1(M146V)  
inhibits monoamine oxidase-A function  
*in vivo* and *in vitro*.**

A Thesis Submitted to the  
College of Graduate Studies and Research  
in Partial Fulfillment of the Requirements  
for a Master's Degree  
in Biological Psychiatry  
Department of Psychiatry  
University of Saskatchewan  
Saskatoon

By  
Lewei Rui

© Copyright Lewei Rui, December 2010. All rights reserved.

## ABSTRACT

Presenilin-1 (PS-1) is the catalytic core of the  $\gamma$ -secretase complex, which is best known for its role in the generation of the Alzheimer disease (AD)-related  $\beta$ -amyloid peptide. Mutated forms of PS-1 are known to be associated with particularly aggressive forms of AD. Changes in monoaminergic neurotransmitter systems, including the serotonin and norepinephrine systems, have long been associated with some of the earliest events in AD, whereas changes in the availability of these same monoamines have historically been associated with clinical depression. Therefore, it is not surprising that depression has now been proposed as a risk factor for developing AD and that pre-demented carriers of mutated forms of PS-1 are more prone to developing depression. The enzyme monoamine oxidase-A (MAO-A) is historically associated with depression and is also a known risk factor for AD. Given this, I hypothesized that MAO-A represents a neurochemical link between depression and AD, and I chose to examine the influence of PS-1 mutations on MAO-A function *in vivo/ex vivo* and *in vitro*.

I first focused on the PS-1(M146V) knock-in mouse model of AD-related PS-1/ $\gamma$ -secretase function. I used a radioenzymatic assay to estimate MAO-A catalytic activity and immunoblot analysis to determine MAO-A protein expression, and found that MAO-A activity does not correlate with MAO-A expression in the cortex and cerebellum of the PS-1(M146V) mice. Furthermore, the potency of the MAO-A inhibitor clorgyline (CLG) is greater in both the cortex and cerebellum of the PS-1(M146V) mice compared to the potency of CLG in wildtype littermates. CLG dose-response curves suggest that there might be a change in cooperativity in the MAO-A protein from PS-1(M146V) cortex (which would suggest a change in conformation and/or access of the substrate to the catalytic pocket in MAO-A). High-pressure liquid chromatography was used to analyze monoamine levels in these same regions. The metabolic profile of monoamines (*i.e.* serotonin, dopamine and norepinephrine) suggests that PS-1(M146V) inhibits MAO-A function in the cortex, but not in the cerebellum. Furthermore, CLG has no significant effect on amine levels in cortex, but tends to increase their accumulation in cerebellum.

The overexpression of PS-1(M146V) in neuronal cultures reveals that this protein

affects MAO-A activity and, more importantly, that PS-1(M146V) co-precipitates with MAO-A, thus suggesting a possibility for a direct protein-protein interaction. This is supported by the observation that MAO-A activity is increased in cell extracts incubated with the PS-1 substrate-competitor, N-[N-(3,5-difluorophenacetyl)-L-alanyl]-S-phenylglycine t-butyl ester (DAPT). Preliminary studies have been undertaken to identify the motif in MAO-A that could be acting as a binding site/target site for PS-1.

These combined results support the hypothesis that PS-1 proteins can influence MAO-A function and, thus, could represent a neurochemical link between depression and AD. Furthermore, MAO-A appears to be a novel interactor for PS-1/ $\gamma$ -secretase. This could well explain some of the ambiguous literature associated with both of these proteins in disorders as diverse as depression and AD.

## ACKNOWLEDGMENTS

First of all, I would like to express my sincere gratitude to my supervisor, Dr. Darrell Mousseau for his continuous professional support and supervision, throughout my Master's program. From the guidance of Dr. Mousseau, I not only developed the technical expertise associated with my project and knowledge of neuropsychiatry, but also learned the way to think independently. Dr. Mousseau is truly an excellent example of a great scientist. His patience and passion on science has always been inspiring and stimulating to me.

I would like to thank the rest of my thesis committee members for their support and guidance: Drs. Adil Nazarali, Paul Wood and Wolfgang Walz. I appreciate their insightful comments and encouragement. I am also thankful to my external examiner, Dr. Jeremy Lee, for his insight and his feedback on this thesis.

Throughout my Master's training, I was most fortunate to work with my fellow graduate students: Geraldine Gabriel, Ji Qi, Tuo Zhao, my colleagues Paul Pennington, Dr. Jennifer Chlan-Fourney and Dr. Zelan Wei. I thank them all for their kind help, stimulating discussions and all the fun we had. I would also like to thank Dr. Glen Baker and his laboratory for the neurochemical (HPLC) analyses. I would like express special thanks to Dr. Zhongjian Jiang, for his patient teaching of the experimental techniques during the first year of my study.

Last but not least, I would like to thank my parents, the rest of family and friends -- they have always been supportive during every day of my 3-year study.

I would like to acknowledge the Scholarships I received from the College of Graduate Studies and Research as well as from the College of Medicine at the University of Saskatchewan. This thesis was supported, in part, by a Laura E. Chapman Award and an Alfred E. Molstad Intramural Award, Department of Psychiatry, University of Saskatchewan.

# TABLE OF CONTENTS

<b>ABSTRACT</b> .....	i
<b>ACKNOWLEDGMENTS</b> .....	iii
<b>LIST OF FIGURES</b> .....	vii
<b>LIST OF TABLES</b> .....	ix
<b>LIST OF ABBREVIATIONS</b> .....	x
<b>1. General Introduction</b> .....	1
1.1 Major Depressive Disorder.....	1
1.1.1 History.....	1
1.1.3 Monoamine-Deficiency hypothesis of depression.....	2
1.2 Monoamine oxidase-A (MAO-A).....	3
1.2.1 Classification of MAO isoforms.....	3
1.2.2 MAO-A structure.....	4
1.2.3 Physiological functions of MAO-A.....	4
1.2.4 MAO-A inhibition and neurodegenerative disease.....	5
1.3 Alzheimer's disease.....	7
1.3.1 Classification and pathophysiology.....	7
1.3.2 The Amyloid hypothesis of AD.....	7
1.4 The $\gamma$ -secretase complex.....	8
1.4.1 An introduction to $\gamma$ -secretase.....	8
1.4.2 Subcellular localization of the PS-1 protein.....	10
1.4.3 $\gamma$ -Secretase signalling.....	11
1.4.4 $\gamma$ -secretase and AD.....	13
1.5 The association between depression and AD.....	16
1.6 Hypothesis.....	16
<b>2. Material and Methods</b> .....	18
2.1 Materials.....	18
2.1.1 Cell lines.....	18
2.1.2 Vectors and plasmids.....	18

2.1.3	Animals.....	23
2.2	Methods.....	23
2.2.1	Cell culture.....	23
2.2.2	Site-directed mutagenesis.....	25
2.2.3	Mini-prep amplification of plasmid DNA.....	26
2.2.4	Maxi-prep amplification of plasmid DNA.....	27
2.2.5	Transformation of bacterial cells.....	28
2.2.6	Transient transfection of mammalian cultures.....	28
2.2.7	Immunoblot/Western Blot assay.....	29
2.2.8	Immunoprecipitation.....	30
2.2.9	MTT conversion assay.....	30
2.2.10	MAO-A activity assay.....	31
2.2.11	Brain regional dissection.....	32
2.2.12	High-pressure liquid chromatography (HPLC).....	32
2.2.13	Immunohistochemistry.....	33
2.1.14	Forced-swim test.....	33
2.1.15	Statistical analyses.....	34
<b>3.</b>	<b>Results.....</b>	<b>35</b>
	<b>Part I: Effects of PS-1 (M146V) variant on MAO-A function in mice.....</b>	<b>35</b>
3.1	MAO-A activity is affected in the PS-1 (M146V) knock-in mice.....	35
3.2	Nissl/thionin staining in wildtype and PS-1 (M146V) mouse sensorimotor cortex .....	36
3.3	The MAO-A inhibitor clorgyline (CLG) exerts behavioural changes in PS- 1(M146V) mice.....	36
3.4	Levels of selected monoamine and acid metabolites in the cortex and cerebellum of wildtype and PS-1(M146V) mice.....	41
3.5	Clorgyline (CLG) is more potent in PS-1 (M146V) mice than in wildtype mice .....	42
3.6	CLG dose-response curves in wildtype and PS-1(M146V) mice.....	42

<b>Part II: Direct interaction between PS-1 and MAO-A proteins in animal and cell extracts.</b> .....	<b>47</b>
3.8 PS-1(M146V) affects Ca <sup>2+</sup> -sensitive MAO-A activity in HT-22 cells. ....	47
3.9 Cell viability of PS-1(M146V)-overexpressing HT-22 cells in the absence and presence of CLG. ....	49
3.10 MAO-A (endogenous and exogenous) co-immunoprecipitates with PS-1 proteins in HT-22 cells.....	49
3.11 DAPT increases MAO-A activity in HT-22 cells and PS-1(M146V) knock-in mice. ....	53
3.12 CLG promotes the interaction between PS-1 and MAO. ....	55
<b>Part III: Mapping the potential motif for interaction between PS-1 and MAO-A</b> .....	<b>57</b>
3.13 Chromatogram sequences of MAO-A A302S and MAO-B S293A. ....	57
3.14 Molecular evidence of the PS-1 targeting motif in MAO-A. ....	60
3.15 MAO-A activity in HT-22 cultures is increased by expression of depression-related PS-1 mutants. ....	60
<b>4. Discussion.</b> .....	<b>63</b>
<b>5. Future directions.</b> .....	<b>63</b>
<u>References</u> .....	<b>70</b>
<b>APPENDIX</b> .....	<b>87</b>

## LIST OF FIGURES

Figure 1.1: 3-D structure of human MAO-A with flavin adenine dinucleotide and clorgyline bound.....	6
Figure 1.2: The amyloid precursor protein (APP) is proteolytically processed by multiple cleavage events.....	9
Figure 1.3: Comparison of APP and Notch processing. ....	12
Figure 1.4. AD-related mutations of the transmembrane protein Presenilin 1. ....	15
Figure 3.1: MAO-A activity with and without Ca <sup>2+</sup> in wildtype and PS-1 (M146V) mice.....	37
Figure 3.2: MAO-A expression in cortex and cerebellum of PS-1(M146V) mice.....	38
Figure 3.3: MAO-A distribution and Nissl staining in wildtype and PS-1(M146V) mice sensorimotor cortex. ....	39
Figure 3.4: MAO-A-sensitive non-cognitive behaviour is revealed in the PS-1(M146V) mice.....	40
Figure 3.5: Cortical and cerebellar levels of indoleamines. ....	43
Figure 3.6: Cortical and cerebellar levels of catecholamines. ....	44
Figure 3.7: The potency of CLG is increased by the PS-1(M146V) protein <i>in vivo</i> .....	45
Figure 3.8: CLG dose-response curve in vehicle-treated wildtype and PS-1(M146V) cortical homogenates. ....	46
Figure 3.9: Overexpression of PS-1 wildtype and PS-1(M146V) affects Ca <sup>2+</sup> -MAO-A activity in HT-22 cells. ....	48
Figure 3.10: MTT reduction in HT-22 cells overexpressing PS-1 proteins. ....	50
Figure 3.11: MAO-A co-immunoprecipitates with PS-1 proteins in cell cultures. ....	52
Figure 3.12: Treatment of PS-1/ $\gamma$ -secretase inhibitor DAPT increases MAO-A activity in HT-22 cells. ....	54



**Figure 3.13: Immunoprecipitation assay for PS-1 and MAO-A in CLG treated/non-CLG-treated PS-1 wildtype or PS-1(M146V) mouse cortex. ....56**

**Figure 3.14: MAO-A contains a putative PS-1 binding site. ....58**

**Figure 3.15: Sequencing of targeted codon substitutions in *MAO-A* and *MAO-B* .....59**

**Figure 3.16: Molecular evidence of a putative PS-1 targeting motif in MAO-A. ....61**

**Figure 3.17: MAO-A activity is increased by overexpression a depression-related PS-1 mutant. ....62**

## **LIST OF TABLES**

<b>Table 2.1: Reagents and commercial sources.....</b>	<b>19</b>
<b>Table 2.2: Company name and address.....</b>	<b>21</b>
<b>Table 2.2: List of Antibodies and the dilution factor. ....</b>	<b>22</b>

## LIST OF ABBREVIATIONS

5-HIAA	5-Hydroxyindoleacetic acid
5-HT	5-Hydroxytryptamine (Serotonin)
A $\beta$	Amyloid- $\beta$
AD	Alzheimer's disease
APH-1	anterior pharynx-defective 1
APP	Amyloid protein precursor
Asp	Aspartic acid
BSA	Bovine serum albumin
CLG	Clorgyline
CTF	C-terminal fragment
DA	Dopamine
DAB	3,3'-Diaminobenzidine
DAPT	N-[N-(3,5-difluorophenacetyl)-L-alanyl]-S-phenylglycine t-butyl ester
DMEM	Dulbecco's modified Eagle's medium
DMSO	Dimethyl sulfoxide
DNA	Deoxyribonucleic acid
<i>E. coli</i>	<i>Escherichia coli</i> (DH5 $\alpha$ strain)
ECL	Enhanced chemiluminescent luminol
ER	Endoplasmic reticulum
FAD	Familial Alzheimer's disease
HEK	Human embryonic kidney cells
HPLC	High performance liquid chromatography
IB	Immunoblot
IP	Immunoprecipitation
LB	Loading buffer
MAO-A	Monoamine oxidase-A
MAO-B	Monoamine oxidase-B
MCS	Multiple cloning site

mRNA	Messenger ribonucleic acid
MTT	3-(4,5-dimethylthiazol-2-yl)-2,5-diphenyltetrazolium bromide
NA	Noradrenaline
NICD	Notch intracellular domain
NTF	N-terminal fragment
PAGE	Polyacrylamide gel electrophoresis
PBS	Phosphate buffered saline
PCR	Polymerase chain reaction
PEA	Phenylethylamine
PEN-2	Presenilin enhancer 2
PS-1/PS-2	Presenilin-1/Presenilin-2
SDS	Sodium dodecyl sulfate
<i>Swe</i>	Swedish (mutation) in the <i>APP</i> gene
TBS/TBS-T	Tris-buffered saline (-Tween 20)
TEMED	N,N,N',N'-tetramethylethylenediamine

## **1. General Introduction.**

### **1.1 Major Depressive Disorder.**

#### **1.1.1 History.**

As early as the 17<sup>th</sup> century, major depression was recognized and known as melancholia, a condition thought to be due to the change of dominant humor in an individual. It was not until the early 19<sup>th</sup> century that the Swiss psychiatrist Adolf Meyer presented the term ‘depression’. He also described a framework that contained both social and biological aspects to emphasize the environment of a person’s life [1, 2]. The first person that associated depression with psychiatric symptoms (in 1865) was Louis Delasiauve, a psychiatrist from France. Around this time, depression was being associated with a low level of physiological emotional function [3] and this new ‘condition’ was more associated with women [4]. In the middle of the 20<sup>th</sup> century, researchers observed that an imbalance of monoamine neurotransmitter in the brain could be induced pharmacologically with compounds such as reserpine, and that this induced depressive symptoms [5]. At the same time, the term Major Depressive Disorder was introduced.

#### **1.1.2 Symptoms and development of depression.**

Major Depressive Disorder is a mental disorder that adversely affects the patient’s family, general health, normal life, including working, sleeping, eating habits and also personal relationships [6]. Depression affects people of all races and does not discriminate between male and female, although females do tend to suffer from depression more than men [7]. In 2009, approximately 9.5% of the population in America, aged 18 and older, suffered from depression, and around 3.4% of this population had suicidal tendencies. Symptoms of depression also include loss of interest in normal activities, low self-esteem, poor memory and problems with concentration [8]. Cognitive symptoms [8] and obvious slowing movements [9] are usually common with older depressed people. In severe cases, the patient may also display symptoms of psychosis, such as delusions and hallucinations, but this is less common [10]. Compared with the aged population, depressed children may show varying symptoms depending on their age [1], and can often display aggression or irritability rather than a low mood [6].

This might explain, in part, why diagnosis could be missed or delayed in children. As stated above, women tend to experience depression more often than men (almost twice as often) [7] and the pattern of symptoms often differs between these two populations, in part due to differences in hormones [11] and the ability to respond to social pressures.

### **1.1.3 Monoamine-Deficiency hypothesis of depression.**

Genetics suggest that complex features, rather than a single gene, are involved in major depression. Serotonin (5-HT)-transporter-linked polymorphic region is a target region that affects transcription of the 5-HT transporter gene. One polymorphism causes the ‘short’ allele, decreases transcription efficiency and results in a decreased expression of the 5-HT transporter. The result is decreased uptake of 5-HT into the presynaptic cells [12, 13] and a potential contribution to depression [14]. Aside from the 5-HT-transporter-linked polymorphic region, no strongly-correlated, specific risk factor for depression has been identified [15]. However, the genome related to a predisposition to depression could be affected epigenetically by environmental factors. For example, Weaver reported that an increase in maternal care by rat dams altered the promoter of the glucocorticoid receptor gene, and this altered the stress responses of their offspring [16].

The monoamine theory of depression is widely accepted as the neurobiological basis for major depression. As early as the 1960s, it was believed that depression was associated with generally low levels of several neurotransmitters, such as serotonin, norepinephrine and dopamine [17, 18]. Blocking monoamine oxidase was one of the first biological mechanisms associated with antidepressant properties and, not surprisingly, the first-generation antidepressants, the tricyclic antidepressants, inhibited the reuptake of these neurotransmitters. Therefore, a deficiency of brain monoaminergic tone clearly plays a critical role in inducing Major Depressive Disorder. This mental disorder could be reversed by agents that increase the availability of brain monoamines [18]. Such agents function by blocking inhibitory presynaptic neuronal metabolism, inhibiting the reuptake of monoamines from the synapse and/or reducing monoamine intraneuronal metabolism [19, 20]. So far, most of the studies related to major depression have been concentrating on the low density of presynaptic monoamine transporter. Apart from this theory, it is also observed that an elevated brain monoamine oxidase-A level can increase the

metabolism of monoamines, which would clearly support why monoamines are usually low in depressed subjects [21]. Among the publications related to monoamine oxidase-A, more tend to focus on the high activity-related allele of the gene for monoamine oxidase-A rather than the protein itself. Theoretically, a higher activity of the monoamine oxidase-A protein could elevate the metabolism of monoamines, such as 5-HT, NE and DA, in much the same way as an increase in the expression of the MAO-A protein would.

## **1.2 Monoamine oxidase-A (MAO-A).**

### **1.2.1 Classification of MAO isoforms.**

Monoamine oxidase is a flavin adenine dinucleotide domain-containing enzyme that is expressed predominantly on the outer membrane of the mitochondria and is widely distributed in all organisms [22]. MAOs catalyze the deamination of monoamines, thus generating aldehydes, and generating reaction byproducts such as hydrogen peroxide and ammonia. Reactive oxygen species can be produced from hydrogen peroxide and can induce damage to the mitochondria and trigger neuronal cell apoptosis [23].

In mammals, two isoforms of MAO are expressed. These isoforms, MAO-A and MAO-B, share approximately 70% identity of primary amino acid sequences [24, 25] and are generally detected, to varying degrees, in most organs [26]. MAO-A is very highly expressed in placenta while MAO-B is the predominant isoform in platelets and lymphocytes [27]. Their distribution also differs in the brain. MAO-A is more abundant in catecholaminergic neurons, while MAO-B is found more often in glial cells as well as in serotonergic and histaminergic neurons [28-30]. Before their molecular characterization, MAOs were often distinguished based on their substrate and inhibitor sensitivity. To some degree, there are overlaps of enzymatic actions for the two isoforms. In most species, they both present a good affinity for dopamine (DA), tryptamine, etc [31]. In rodent brain, MAO-A is the main enzyme for DA degradation, while in human brain, MAO-B is the main enzyme for DA oxidation [32]. Generally, MAO-A has a high affinity for serotonin (5-HT) and norepinephrine (NE), whereas MAO-B prefers  $\beta$ -phenylethylamine (PEA) [33]. Therefore, in most cases, 5-HT levels can be enhanced by inhibition of MAO-A, but not MAO-B. However, exceptions to this rule could happen, for example, depending on the change of substrate/enzyme concentration (i.e. the

respective isoforms will oxidize the other's substrate if enough of the substrate is available or if the particular isoform is not expressed at sufficiently high levels) [34].

The two isoenzymes can also be characterized pharmacologically. MAO-A is sensitive to the selective inhibitor clorgyline [35], while MAO-B is blocked by low concentration of L-deprenyl [36]. Recently, many researchers have focused on developing different types of MAO inhibitors and have put effort into studying their pharmaceutical effects in mental disorders, such as depression and Alzheimer's disease. This will be discussed in the following sections.

### **1.2.2 MAO-A structure.**

The primary amino acid sequence of MAO-A is highly important for its catalytic activity. In the molecule, there is a conservative sequence consisting of Ser-Gly-Gly-Cys-Tyr, which binds the flavin adenine dinucleotide cofactor [37], and mutagenesis studies have shown that amino acids 152-366 are critical for inhibitor and substrate binding [38, 39]. The 3D-structure of MAO-A has been studied and modeled in recent years [40, 41] (Figure 1.1). Edmondson's research group provided a nice representation of the three dimensional structure of MAO-A [42]. They also compared structures of human MAO-A (hMAO-A) and rat MAO-A (rMAO-A). Although the primary sequence of hMAO is quite similar to that of the rat, their catalytic sites differ. Crystallography suggests that, unlike the dimer-form of rMAO-A and hMAO-B, hMAO-A's active domain contains a single hydrophobic cavity-shaping loop (residues 210-216), which has a larger volume than rMAO-A's, and, in contrast to rMAO-A, hMAO-A works as a monomer [42]. The conformation of the cavity is controlled by the formation of dimer in rMAO-A. Therefore, despite hMAO-A and rMAO-A having 92% sequence identity, hMAO-A exhibits a 10-times lower affinity for its selective inhibitor clorgyline than does rMAO-A [39].

### **1.2.3 Physiological functions of MAO-A.**

The physiological functions of MAO-A are slightly different in peripheral tissues than in the brain. In tissues such as liver and lungs, MAO-A exerts protective effects by removing dietary amines from the blood [43]. In the central nervous system, MAO-A is



important in monoamine neurotransmitter metabolism in the nerve terminals, and also in preventing excessive release of these neurotransmitters from the glial cells. It is known that serotonergic neurons have a relatively low expression of MAO-A, but high expression of MAO-B. This indicated that glial cells could play a very important role in degrading 5-HT. Indeed, only inhibition of MAO-A, but not MAO-B, can dramatically increase the levels of 5-HT and also exert antidepressant effects [43]. MAO-B in the neurons might only target foreign amines and, thus, limit their entry into synaptic vesicles.

MAO-A has been linked with aggressive behaviour [44]. Indeed, disruption of the *mao-A* gene by insertional mutagenesis in a mouse model results in a dramatic increase of 5-HT and NE, but only a modest elevation of DA. Not surprisingly, loss of MAO-A in this mouse strain leads to aggressive behaviour [44, 45], which resembles the aggressive phenotype seen in a human kindred with a deletion in the *MAO-A* gene (affected males exhibit borderline intelligence and pathologic impulsive aggression) [46, 47]. MAO-A knock-out mice also appear to have a better fear-related memory [48, 49], whereas MAO-A deficiency in rodent usually induces an enhanced resistance to environmental stress [44].

#### **1.2.4 MAO-A inhibition and neurodegenerative disease.**

MAO-A inhibitors (MAOIs) were the first developed antidepressants and are a class of powerful drugs to treat depressive disorder. A significant elevation of 5-HT and NE can be observed after MAOI treatment [50]. It has been reported that due to the “cheese effect” associated with these compounds (an effect due to a significant increase in circulating dietary tyramine (from foodstuffs such as aged cheese, hence the name, and wine) resulting from inhibition of gut wall MAO) [51], MAOIs should be prescribed as a second choice for depressed patients, only after 5-HT reuptake inhibitors have been tried. Recently-developed reversible MAO-A inhibitors such as moclobemide [52] and brofaromine [53] are particularly efficacious in refractory depression [54-56]. Studies have now shown that depression can promote cognitive impairment and that it is a potential risk factor for Alzheimer’s disease [57]. Hydrogen peroxide (H<sub>2</sub>O<sub>2</sub>), as a natural by-product of MAO-mediated metabolism, can contribute to ROS formation and trigger



**Figure 1.1: 3-D structure of human MAO-A with flavin adenine dinucleotide and clorgyline bound.** The monomer is depicted using ribbons. MAO-A is attached to the outer membrane (depicted as a light green strip) of mitochondria (the C-terminal membrane region is highlighted in green and is anchored to the membrane). The flavin adenine dinucleotide-binding domain is highlighted in blue. The MAO-A inhibitor clorgyline is located in the very center of the structure and is represented by the green, black and white spheres. (Image used with permission, from ref [42])

mitochondrial damage leading to neuronal cell death [23]. Therefore, it is not surprising that MAO-A inhibition can also be an effective treatment in neurodegenerative diseases such as Parkinson disease, Huntington's disease and Alzheimer's disease [20]. As my thesis focuses MAO in Alzheimer's disease, the literature review will focus more on Alzheimer's disease.

### **1.3 Alzheimer's disease.**

#### **1.3.1 Classification and pathophysiology.**

Alzheimer's disease (AD) is named for the German psychiatrist who first described the disease and its neuropathology in 1906. It is now recognized as one of the most prevalent neurodegenerative diseases related to aging with an incidence of approximately 5%-10% of the population above 65 years of age [58]. The pathological changes include neuronal degeneration (most obvious in cerebral cortex and hippocampus), the intracellular neurofibrillary tangle (NFT) and the extracellular senile plaque [59]. Memory loss and dementia are two manifestations in the disease. Phosphorylation of the Tau protein is key to NFT formation while aggregated  $\beta$ -amyloid peptide ( $A\beta$ ) is the central component of senile plaque [59]. Deposition of  $A\beta$  leads to oxidative stress, apoptosis, or abnormal growth of axon as well as enhancing NFT formation [60].

Types of AD include late-onset (also named sporadic AD) and early-onset (or familial) AD (FAD). Late-onset AD is the most common form of the disease. The likelihood for people getting the disease doubles every 5 years after the age of 65 and affects more than 30% of people aged 85 and over [58]. The early-onset form of the disease is less common than sporadic AD and often affects less than 10% of AD patients. Early-onset AD is mainly associated with three mutant genes, presenilin-1 (PS-1), presenilin-2 (PS-2) and amyloid protein precursor (APP). In some extremely aggressive cases of FAD, people may develop AD in their late 20s and early 30s [61].

#### **1.3.2 The Amyloid hypothesis of AD.**

Deposition of  $A\beta$  in the wall of cerebral blood vessels is the most important feature of AD. The  $A\beta$  peptide can contain between 39 to 43 amino acids and is

generated from the cleavage product of transmembrane APP [62]. APP is expressed in all types of cells and although the function of APP in peripheral system remains unclear, it has been associated with synapse formation as well as neuronal migration in the brain [63, 64]. Three enzymes,  $\alpha$ -,  $\beta$ -, and  $\gamma$ -secretase are involved in two pathways associated with the APP cleavage process (Figure 1.2). In the ‘non-amyloidogenic’ pathway, APP is first cleaved by  $\alpha$ -secretase between residues 16 and 17 of the A $\beta$  peptide; this effectively inhibits A $\beta$  formation and releases the soluble  $\alpha$ -site cleavage product sAPP $\alpha$  [65]. Mutations in the APP protein that have been associated with AD often are localized near the  $\beta$ -secretase site and facilitate the cleavage by  $\beta$ -secretase and the release of the A $\beta$  peptide.  $\beta$ -secretase cleaves APP between residues 596 and 597, thus producing the C-terminus of APP, referred to as C99 [66]. The membrane-bound C99 fragment is further cleaved by  $\gamma$ -secretase between residues 637 and 639 to release the full length A $\beta$  peptide [67]. Different lengths of A $\beta$  monomers can be produced following the proteolytic processing because  $\gamma$ -secretase is able to cut APP at different sites. However, 39-42-mers of A $\beta$  appear to be the major forms of A $\beta$  in plaques in the brain of AD patients [68].

#### **1.4 The $\gamma$ -secretase complex.**

##### **1.4.1 An introduction to $\gamma$ -secretase.**

The intramembrane proteolysis of Type I transmembrane proteins by the  $\gamma$ -secretase complex is an evolutionarily conserved biochemical process in most mammals [69]. Four components have been identified in this membrane-bound complex; these are presenilin, nicastrin, APH-1 and PEN-2 [70]. Researchers first recognized  $\gamma$ -secretase because of its intramembrane-cleaving function during the processing of A $\beta$  in AD [60]. As mentioned above,  $\gamma$ -secretase acts as a key enzyme during the cleavage of APP and produces A $\beta$ -40/42-mers. In addition to its role in AD, during nervous system development and neuronal outgrowth,  $\gamma$ -secretase also serves as an important mediator in the Notch signaling pathway [71]. Following cleavage by  $\gamma$ -secretase, the intracellular domain of the Notch receptor is released from the cell membrane and translocates to the nucleus, where it regulates a number of genes [72, 73]. Therefore,  $\gamma$ -secretase normally

plays a crucial role in diverse signal transduction events.

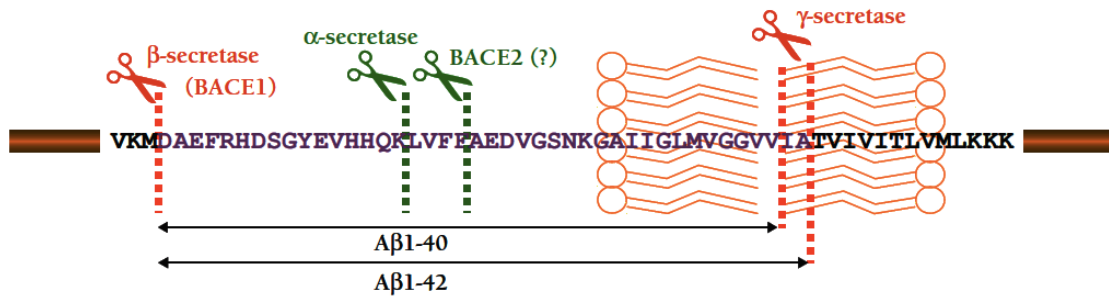


**Figure 1.2: The amyloid precursor protein (APP) is proteolytically processed by multiple cleavage events.** APP is cleaved by the  $\beta$ - and  $\gamma$ -secretase enzyme complexes sequentially to release the  $A\beta(1-40)$  and/or  $A\beta(1-42)$  fragments. These fragments are thought to contribute to the pathological progression of AD. Under non-pathological conditions, APP is cleaved by  $\alpha$ -secretase or BACE-2 ( $\beta$ -site APP-cleaving enzyme 2), thus precluding the release of the amyloidogenic and toxic  $A\beta$  fragment. (Image used with permission, from ref [74])

Presenilin-1 (PS) is known as the central catalytic component of the  $\gamma$ -secretase complex [59]. PS is an eight-domain transmembrane protein and it is endoproteolytically cleaved within the cytoplasmic loop to generate an N-terminal fragment (NTF) and a smaller C-terminal fragment (CTF) [75]. These two fragments of PS-1 remain associated *in vivo* and it is this heterodimeric conformation that mediates  $\gamma$ -secretase's catalytic activity [75]. PS-1 is now well known to be involved in both normal and abnormal biological processes. The  $\gamma$ -secretase activity can be interfered by several substitutions within the PS protein, *i.e.* aspartate 257 (D257) or by the deletion of exon9 in PS-1 (the deletion of exon 9 precludes the endoproteolytic processing of the PS-1 protein) [76, 77]. The aspartate 257 (D257) and D385 residues are very important for the function of the complex and are central to substrate recognition. Although PS-1 is indispensable to the function of the  $\gamma$ -secretase complex, overexpressing PS-1 alone does not increase  $\gamma$ -secretase activity [73], which suggests that the function of PS-1 and its expression level are tightly controlled by other co-factors. Recent research indicates that nicastrin is one of the potential limiting factors for  $\gamma$ -secretase activity, and nicastrin exerts its influence by associating directly with PS-1 [78]. However, co-expression studies quickly revealed that  $\gamma$ -secretase function is not solely dependent on these two proteins [79], and two other proteins identified as APH-1 and PEN-2 are now known to be essential factors for PS-1 endoproteolysis and for  $\gamma$ -secretase activity [73].

#### **1.4.2 Subcellular localization of the PS-1 protein.**

PS-1/ $\gamma$ -secretase is expressed widely on numerous cellular organelles, including the endoplasmic reticulum (ER), the plasma membrane, the nuclear envelope, and lysosomal membranes [80-82]. PS-1 has been detected in the Golgi complex [83, 84], but whether PS-1 exists on the Golgi membrane is still under dispute.

Recently, a group from Sweden reported, based on their immunoelectron microscopy study and subcellular analysis, that active PS-1 also localizes to the mitochondrial membranes [85, 86]. Although the function of PS-1/ $\gamma$ -secretase in mitochondria is unknown, this does open up the intriguing possibility that PS-1 is exerting effects on an organelle that is not its usual location within the cell, *i.e.* the

endoplasmic reticulum. Knowing the subcellular localization of PS-1 will help to understand more about the function of this enzyme complex function and about its interaction with other proteins. More recently, Area-Gomez and colleagues reported that presenilins are enriched in endoplasmic reticulum membranes, particularly the portion of the membrane that is in close proximity to mitochondria [86]. Thus, a biochemical link as well as a physical link allows for protein-protein interactions between the endoplasmic reticulum and mitochondria, which in turn allows for inter-organelle communication and protein trafficking [87].

### 1.4.3 $\gamma$ -Secretase signalling.

Two evolutionally conserved aspartate residues, D257 and D385 (located on PS-1), play a crucial role in  $\gamma$ -secretase function [77]. Currently, APP and Notch are the two best known substrates to have been associated with  $\gamma$ -secretase cleavage. Processing of APP was described above. The Notch signaling pathway is involved with cell fate decision during both embryonic and adult life, and reduction of Notch signaling can be observed in PS-1 knock-out animals [74]. The Notch pathway is highly conserved across most multi-cellular organisms [88] and Notch undergoes a similar cleavage process as described above for APP (Figure 1.3). The transduction pathway includes three components: ligand, intracellular Notch receptor and transcription factors [89]. The *notch* gene family encodes different types of Notch receptors, which interact mainly with five ligands (JAG1, JAG2, and three Delta-like ligands) [90]. Following the interaction with ligands on the plasma membrane, Notch is cleaved by the ADAM (a disintegrin and metalloprotease) family of metalloproteases [88] and the membrane-bound fragment can subsequently be cleaved by PS-1/ $\gamma$ -secretase. The resulting fragment, termed the Notch intracellular domain (NICD), can translocate to the nucleus (in much the same way as the analogous APP fragment can, as discussed above) and target transcriptional factors such as CSL [91]. Binding with Notch, CSL can convert from transcriptional suppressor to an activator, and then induce a series of downstream events. Presenilins are required for both APP and Notch proteolysis. Therefore, these two events can be both blocked by PS/ $\gamma$ -secretase inhibitors. Not surprisingly, inhibition of this protease as a therapy to treat AD must interfere the normal Notch signaling and has not led to any significant therapeutic

benefit.

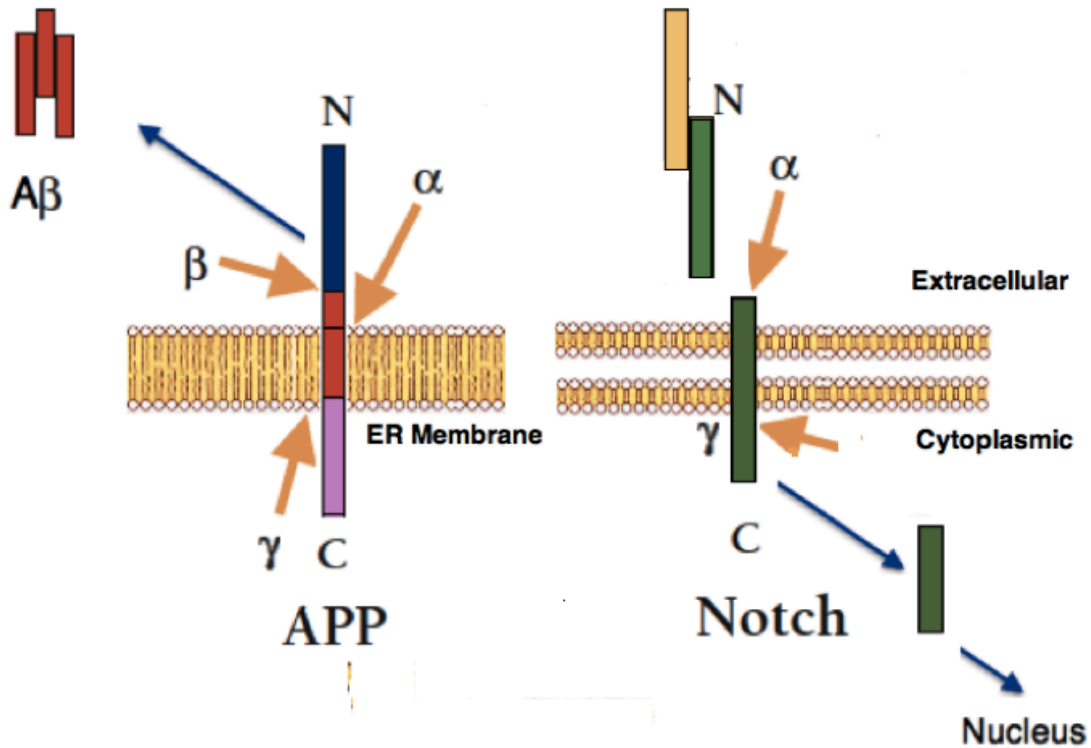


**Figure 1.3: Comparison of APP and Notch processing.** The APP protein and the Notch receptor are cleaved by  $\beta$ -secretase and  $\alpha$ -secretase respectively to give rise to different N-terminal fragments. Then both of the proteins are processed by  $\gamma$ -secretase and generate the intracellular C-terminal fragments. The A $\beta$  fragment is generated at the ER and is secreted to the outside of the cell. The Notch receptor is processed at the plasma membrane; the N-terminal portion mediates cell-cell communication and the C-terminal fragment translocates to the nucleus.



#### 1.4.4 $\gamma$ -secretase and AD.

##### 1.4.4.1 PS-1 mutants and AD.

The *APP* gene was the first factor linked to familial AD [92]. However, soon afterwards the demonstration of mutations in the *PSEN1* gene also were shown to contribute to familial Alzheimer's disease (FAD) [93, 94] and now more than 160 PS-1 mutations as well as 10 PS-2 mutations have been identified [95]. Most of these mutations in both of the PS homologues are localized within the transmembrane domain or in the large intracellular loop, which has been identified as the  $\gamma$ -secretase catalytic core (Figure 1.4) [96]. Compared with PS-2, PS-1 is much more causally linked to AD. PS-1 is a 467 amino acid membrane binding protein with 8 or 9 transmembrane domain (Figure 1.4). Genetic and functional studies of AD have revealed that PS-1 mutations and their effects on  $\gamma$ -secretase function play a central role in AD pathobiology [97]. Compared to the other genetic factors (*APP* and *PSEN-2*), the onset age of PS-1-linked FAD mutations has been observed to be the earliest, starting as early as late teens [98]. Therefore, mutated PS-1 and its pathological function have attracted the most attention to-date. Of interest to this thesis work is the fact that carriers of mutated forms of PS-1 tend to be more prone to developing depression (well before they demonstrate any signs of dementia) than their non-carrier siblings [99, 100].

Among the many PS-1 mutations, approximately 40 of them have been associated with FAD/early-onset AD (age of onset: 28-60). Most of these mutations are missense mutations (one amino acid is substituted because of a single nucleotide difference in the gene) except an in-frame deletion of exon9 ( $\Delta$ Ex9) [95]. It has been suggested that expression of PS-1( $\Delta$ Ex9) leads to an increasing amount of N- and C- terminal fragments by partially blocking the full-length PS-1 degradation [101]. A hypothesis was derived that the deletion of exon9, through a dominant-negative mechanism, would cause a gain in dysfunction rather than a simple loss of function [102]. Furthermore, the PS-1( $\Delta$ Ex9) mutation also gives the highest level of A $\beta$ 42 [78], but the mechanism used to generate this A $\beta$  peptide has yet to be determined.

The PS-1(M146V) missense mutation is frequently studied in the laboratory. The age of onset of AD in carriers of this mutation is between 36-40 years of age [103]. Aside

from altering APP processing, this mutant can increase the proteolysis of the p75 receptor (which has been associated with the death of cholinergic neurons) in the pre-neuronal PC12 cell line, [104], whereas a PS-1(M146V) knock-in mouse displays increased calcium dysregulation and mitochondrial oxidative stress [105-107].

#### 1.4.4.2 Inhibition of $\gamma$ -secretase.

Currently, overproduction of A $\beta$  generated through sequential cleavage by  $\beta$ - and  $\gamma$ -secretases provides the most compelling support for the amyloid hypothesis for AD. A great number of FAD mutation cases are related to the *PSEN-1* gene. It is known that FAD shares a common disease progression with late-onset AD, therefore, PS-1 has become an important target for therapy in both types of AD. However, in addition to APP,  $\gamma$ -secretase is also involved with the processing of a number of other substrates [108]. It is unclear exactly which substrates might be altered by generalized targeting of PS-1; however, unwanted inhibition of the Notch signalling pathway by  $\gamma$ -secretase inhibitors is the major side effect and challenge in animal research [109]. Experimentally, homozygous knockout of PS-1 is embryonic-lethal in mice [109], whereas animals treated with  $\gamma$ -secretase inhibitors often die from intestinal cell hyperplasia as well as spleen atrophy [110]. Therefore, an APP-specific inhibitor, i.e. one that targets only APP processing by this enzyme complex, is needed for optimal treatment of AD.

The semi-peptidic DAPT [N-[N-(3,5-difluorophenacetyl)-L-alanyl]-S-phenylglycine t-butyl ester] is the first  $\gamma$ -secretase inhibitor studied *in vivo*. It is reported that A $\beta$  production could be dose-dependently reduced by DAPT in both plasma and cortex [111, 112]. However, in 17-month-old mice, DAPT can reduce A $\beta$ , but not in the brain. Yet, these aged mice have shown an improvement in cognitive function [113]. Besides, LY-411575 [112] and LY-450139 [114] are the two other orally active inhibitors for blocking  $\gamma$ -secretase *in vivo*. The former was reported to reduce A $\beta$ <sub>40/42</sub> in both hippocampus and cortex, while the latter has been tested in human phase II trial [112]. No apparent Notch-related side effects were observed with LY-450139 [114]. Therefore, this suggests that this compound is possible as a therapeutic inhibitor in AD as it would only targeting the A $\beta$ -related  $\gamma$ -secretase function.

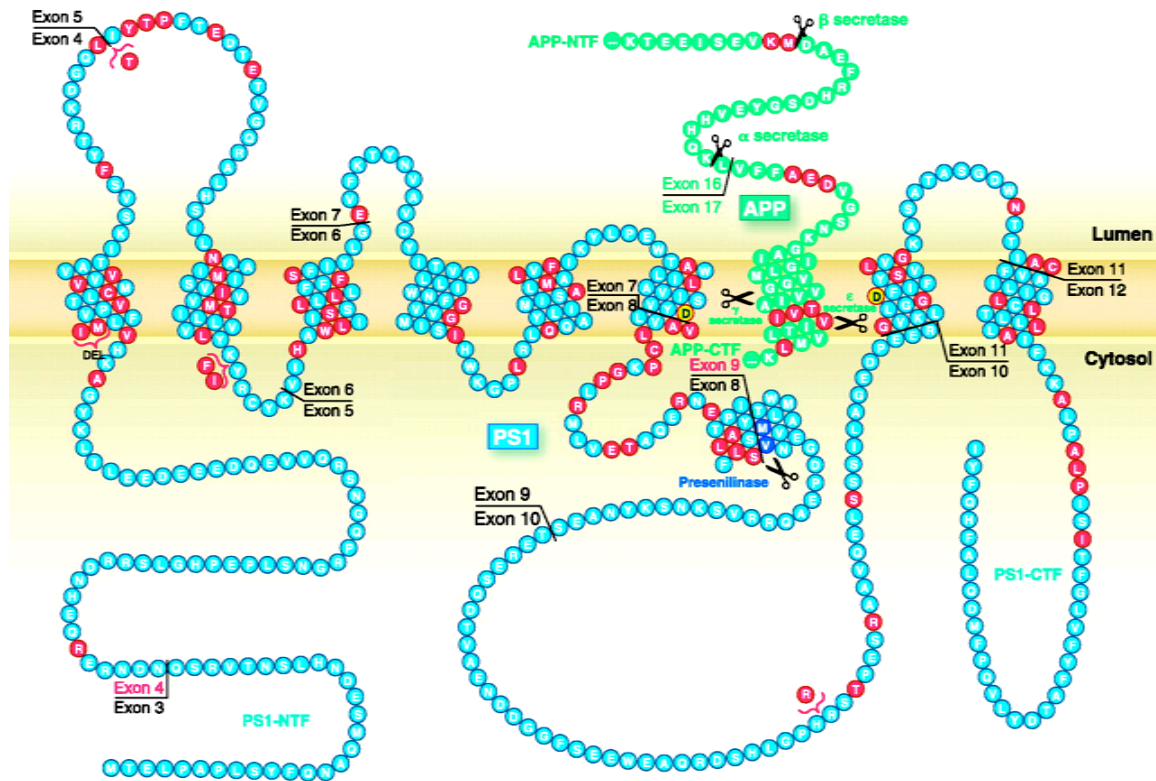


**Figure 1.4. AD-related mutations of the transmembrane protein Presenilin 1.** Approximately 160 mutations (red) are noted in PS-1 protein (blue circles); Two aspartate residues, D257 and D385, within the PS-1 protein that are integral for substrate recognition are highlighted in yellow. The region between transmembrane domain six and seven is the substrate cleavage core that is central to  $\gamma$ -secretase function. The 'scissors' icons along APP (green circles) indicate sites of secretase-mediated cleavage. The 'scissors' icons close to the junction of Exon8 and Exon9 of PS-1 indicate where PS-1 is endoproteolytically processed. (Image used with permission, from ref [115])

## 1.5 The association between depression and AD.

As early as 1996, early mood changes, including depression, had been found to be common in AD [2]. Neurochemical changes, particularly with monoamines such as serotonin and noradrenaline, have long been associated with some of the earliest events in AD [60]. Because the main substrate of MAO-A, *i.e.* serotonin/5-HT, is implicated in major depression, MAO-A is a critical target for the treatment of clinical depression, and it is also thought to contribute to oxidative stress through the production of H<sub>2</sub>O<sub>2</sub> as a natural by-product of monoamine degradation. With this in mind, perhaps it is reasonable that some of the most vulnerable cells in the AD brain are MAO-A-immunoreactive cells [116]. Furthermore, region-specific noradrenergic and serotonergic degeneration occurs in earlier stages of AD [117, 118] and MAO-A/MAO-B expression is highly abundant in these two systems of the brain. It has recently been noticed that not only MAO-A, but also PS-1, and all other  $\gamma$ -secretase components, could be detected in mitochondria [85]. The proximity of the endoplasmic reticulum (where  $\gamma$ -secretase is normally expressed) to the mitochondria is spatially convenient for the interaction between MAO-A and PS-1. Since the symptoms of AD only present many years after the cellular changes, it is possible that MAO-A, as a key enzyme in depression, may also mediate the early neurochemical changes occurring in AD. Both depression [119] and MAO-A [120-124] are now acknowledged risk factors for AD.

## 1.6 Hypothesis.

$\gamma$ -Secretase plays a key role in AD. PS-1 is the catalytic core of the  $\gamma$ -secretase complex. Mutated forms of PS-1 have been associated with particularly aggressive [*i.e.* early-onset] forms of AD and some of these mutations have also been associated with depression in pre-demented AD patients suggesting that depression and AD might share a common causative mechanism. The enzyme MAO-A is historically associated with depression and is also a known risk factor for AD. I propose that MAO-A is a shared factor in these two pathologies.

To better understand the function of PS-1-linked FAD mutations, this project uses the PS-1(M146V) knock-in mouse and uses transient expression of the PS-1(M146V)

protein in neuronal cells (e.g. HT-22 and N2a). The PS-1(M146V) variant is very aggressive and is able to cause AD at a mean of 39 years of age [125]. PS-1(M146V) increases the level of A $\beta$  in transgenic mice [126].

Based on the facts outlined in my review of the literature, I hypothesize that PS-1 can regulate MAO activity and that this contributes to the neurochemical changes associated with AD-related pathology. In this project, the influence of PS-1(M146V) on MAO-A function was examined both in *vivo/ex vivo* and *in vitro*.

**The specific aims of this thesis were:**

- a. To determine if MAO-A function is affected in PS-1(M146V) knock-in animals as well as in PS-1(M146V) overexpressing cells;
- b. To determine whether there are any behavioural and MAO-A-related neurochemical changes in PS-1(M146V) knock-in mice;
- c. To determine whether pharmacological inhibition of MAO-A can exert an effect in a PS-1(M146V) background *in vivo* and *in vitro*;
- d. To determine whether MAO-A and PS-1 proteins interact;
- e. And, finally, if (d) proves to be true, then identify the potential motif that could mediate the interaction between PS-1 and MAO-A.

## **2. Material and Methods.**

### **2.1 Materials.**

All materials and reagent used in the experiment below were obtained from commercial sources (Table 2.1). The addresses of each company are listed in Table 2.2.

The competent cells were generated from DH5 $\alpha$  *E. coli* bacterial strain (ATCC). They were used for plasmid transformation. Three antibodies used are listed in Table 2.3.

#### **2.1.1 Cell lines.**

Mouse hippocampal-derived HT-22 cells (provided by Dr. P. Maher, The Scripps Research Institute, La Jolla, CA) and murine neuroblastoma cells (N2a) (ATCC) were used in the following experiments. The characteristics of these two cell lines allow for the investigation of the various aspects of MAO-A protein. Both HT-22 and N2a cells are neuronal cell lines. Using of HT-22 cells allows us to study the effect of PS-1 protein on *endogenous* MAO-A function due to the high basal MAO-A activity in this cell line. In contrast, we used N2a cell to examine the interaction between PS-1 and *overexpressed* MAO-A, as this cell line has low MAO-A activity as well as low MAO-A protein expression.

#### **2.1.2 Vectors and plasmids.**

Plasmid pcDNA3.1(+) (Invitrogen) and pCMV/myc/mito were used in some of the experiments involving transient transfection. The Immediate-early Cytomegalovirus virus (CMV) promoter in the pcDNA3.1(+) plasmid vector confers a high level expression in a wide variety of mammalian cells. The multiple cloning site (MCS) allows directed insertion of cDNA and the Ampicillin antibiotic resistance gene allows for selection of clones (e.g. only those cells that have the plasmid, and Ampicillin resistance, will survive in medium to which Ampicillin has been added). pcDNA3.1(+) is useful for studying post-translational modification of the target protein. In this thesis, pCMV/myc/mito was used for subcloning all of the MAO-A substitution mutants, all of which are targeted (by virtue of a specific targeting sequence) to the mitochondria; this plasmid also has the specific MCS and Ampicillin resistance gene.

<b>Reagent</b>	<b>Company</b>
DH5 $\alpha$ <i>E. coli</i>	American Type Culture Collection
N2a	American Type Culture Collection
pcDNA3.1(+); pCMV/myc/mito	Invitrogen
DMEM	GIBCO-BRL
FBS	GIBCO-BRL
F-12 (Kaighn's Modification)	Hyclone
Rat-tail collagen	BD-Bioscience
Trypsin-EDTA	Sigma-Aldrich
Cell Freezing Media	GIBCO-BRL
Bacto Tryptone	BD Biosciences
Bacto Yeast Extract	BD Biosciences
MgCl <sub>2</sub>	EM Science Inc.
Glucose	BDH Inc.
EDTA	EMD Chemical Inc.
Tris-base	J. T. Baker
NaOH	EMD Chemical Inc.
Lipofectamine 2000	Invitrogen
OPTI-MEM	GIBCO-BRL
Protease inhibitor cocktail	Sigma-Aldrich
BCA protein assay kit	Pierce
Mercaptoethanol	EM Science Inc
Bromophenol blue	Sigma-Aldrich
Tris-HCL	ICN Biomedicals
Acrylamide	Bio-rad Laboratories
LiCl	EMD Chemical Inc.
Tris-base	J.T. Baker
Glycine	MP Biomedicals

Nitrocellulose membrane	Bio-rad Laboratories
Quikchange® Site-Directed Mutagenesis Kit	Stratagene
Tween 20	Sigma-Aldrich
Bovine Serum Albumin	Sigma-Aldrich
Triton-X 100	Sigma-Aldrich
Glycerol	Biomedicals
Ethyl acetate	BDH Inc.
DAPT	Sigma-Aldrich
ECL	Amersham Biosciences
ACS Scintillation	CocktailAmersham Biosciences
Sepharose-A/G	GE Healthcare
DMSO	EM Science Inc.
[ <sup>14</sup> C]-labeled serotonin	Perkin Elmer

**Table 2.1 Reagents and commercial sources.**



<b>Company</b>	<b>Address</b>
<b>American type culture collection</b>	Manassas, VA, USA
<b>BD biosciences</b>	Mississauga, ON, Canada
<b>BDH Inc.</b>	Toronto, ON, Canada
<b>Bio-Rad</b>	Hercules, CA, USA
<b>Cell Signaling Technology</b>	Danvers, MA, USA
<b>EM Science Inc.</b>	Gibbstown, NJ, USA
<b>EMD Biosciences Inc.</b>	San Diego, CA, USA
<b>EMD Chemicals Inc.</b>	Gibbstown, NJ, USA
<b>Fermentas Inc</b>	Burlington, ON, Canada
<b>GE Healthcare</b>	Uppsala, Sweden
<b>GIBCO-BRL</b>	Gaithersburg, MD, USA
<b>Hyclone</b>	Logan, UT, USA
<b>Invitrogen</b>	Carlsbad, CA, USA
<b>PerkinElmer</b>	Waltham, MA, USA
<b>Pierce</b>	Rockford, IL, USA
<b>Santa Cruz Biotechnology</b>	Santa Cruz, CA, USA
<b>Sigma-Aldrich</b>	St. Louis, MO, USA
<b>The Jackson Laboratory</b>	Bar Harbor, ME, USA
<b>VWR</b>	West Chester, PA, USA

**Table 2.2      Company name and address.**

<b>Primary Antibody</b>	<b>Dilution</b>	<b>Supplier</b>
<b>MAO-A (H-70)</b>	1:1000	Santa Cruz Biotech
<b>C-Myc</b>	1:500	Santa Cruz Biotech
<b>FLAG</b>	1:500	Sigma-Aldrich
<b><math>\beta</math>-Actin</b>	1:3000	Sigma-Aldrich
<b>PS-1-loop</b>	1:1000	(CHEMICON International)
<b>Secondary Antibody</b>	<b>Dilution</b>	<b>Supplier</b>
<b>Donkey Anti-Goat IgG</b>	1:2000	Santa Cruz Biotech
<b>Goat Anti-Rabbit IgG</b>	1:2000	Cedarlane Laboratories
<b>Goat Anti-Mouse IgG</b>	1:2000	Cedarlane Laboratories

**Table 2.3 List of antibodies, dilutions and suppliers.**

MAO-A/B cDNA were amplified in the pCMV/myc/mito and pcDNA3.1 (+) mammalian expression vectors. Based on multiple sequence alignment and identification of a potential motif that mediates the interaction between PS-1 and MAO-A, wildtype MAO-A cDNA was then used to generate the substitutions within this motif, e.g. A302S. The complementary sequence in MAO-B cDNA was used to generate the S293A mutant (so that it resembled the motif in MAO-A).

### **2.1.3 Animals.**

Knock-in mice (M146V) overexpressing human PS-1 mutant were purchased from the Jackson Laboratory. The transgene contains a mouse Thy1 promoter that drives the expression of human PS-1 with the amino acid substitution of Valine (V) for Methionine (M) at position 146 (M146V). The homozygous and wildtype lines were obtained from crossing heterozygous mice. Genotypes were routinely confirmed by PCR and restriction analysis (Figure.2.1). Because of the dominant effect of the transgene, hetero- and homozygous mice were pooled for the purposes of these studies.

Animals were housed in a 12h light/dark cycle at 20°C. Food and water were available *ad libitum*. Each procedure was followed within the guidelines established by the Canadian Council on Animal Care and approved by the University of Saskatchewan Committee on Animal Care and Supply.

## **2.2 Methods.**

### **2.2.1 Cell culture.**

Cells were cultured in 10 cm Falcon tissue culture plates and incubated at 37°C, under 5% CO<sub>2</sub> atmosphere. Except for the PC12 cell line, all cell lines were cultured in low glucose Dulbecco's Modified Eagle's Medium (DMEM) with 10% fetal bovine serum. The medium for PC12 cells is supplemented with 15% horse serum and 2.5% fetal bovine serum (FBS) in Ham's F-12 (Kaighn's Modification) medium. The culture plates for PC12 cells were pre-coated with rat-tail collagen to enhance cell adhesion.

For adherent cultures including HT-22 and HEK, medium was removed and discarded and the cells were rinsed with a balanced salt solution (PBS). Cells were washed by gently rocking the plate and then discarding the washing solution. Cells were

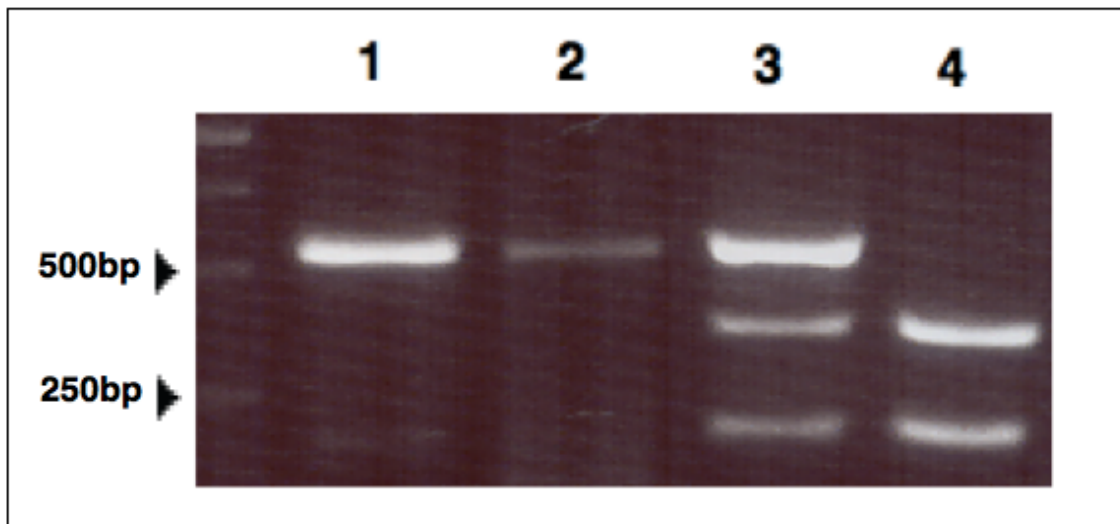


**Figure 2.1: Genotyping of the PS-1(M146V) mice.** Genomic DNA was extracted from tail snips. The PS-1 gene was first amplified by PCR and then digested with the restriction enzyme *Eco 9II* (note that the mutation in the codon that leads to the M-to-V substitution introduces an *Eco 9II* restriction site). Lane 1 and 2 are wildtype mice (no mutation, so no restriction by *Eco 9II*). Lane 3 has an unrestricted band (wildtype) and two smaller bands (a restricted allele), which indicates it is a heterozygous mouse. Note that as the two lower bands (in Lane 3) are restricted fragments of the upper band, that their combined ‘weight’ is equal to that of the upper band. Lane 4 has no wildtype band, but has the two lower ‘restricted’ bands, which indicates it is a homozygous mouse.

detached by incubating with Trypsin-EDTA at 37°C for 2-3 min. Equal volumes of culture medium were added to terminate the digestion. The detached cells were resuspended in complete growth medium by pipetting repeatedly over the surface. The cells were then passaged to new plates and returned to 37°C in the 5% CO<sub>2</sub> atmosphere humidified incubator. Cell stock, when needed, was made using Cell Freezing Media, and the cells were then stored in liquid nitrogen.

### 2.2.2 Site-directed mutagenesis.

All of the mutants were generated using the Quikchange® Site-Directed Mutagenesis Kit. The MAO-A A302S (Alanine to Serine) mutant was generated from the wildtype MAO-A cDNA that had been subcloned into the pCMV/myc/mito mammalian expression vector. MAO-B S293A (Serine to Alanine) was generated from the corresponding wildtype MAO-B-myc cDNA.

All pairs of primers for use in the amino acid substitution are designed individually according to the PCR based site-directed mutagenesis protocol (*i.e.* length and GC content).

The primers were as follows (mutated codons are underlined and highlighted in red):

For the MAO-A A302S substitution:

Forward: 5'-TT CCA ATG GGA TCT GTC ATT AAG TGC ATG-3'

Reverse: 3'-CAT GCA CTT AAT GAC AGA TCC CAT TGG AAG-5'

For the MAO-B S293A substitution:

Forward: 5'-ACT CGT GTG CCT TTG GGT GCA GTC ATC AAG TGT ATA G-3'

Reverse: 3'-TAT ACA CTT GAT GAC TGC ACC CAA AGG CAC ACG AG-5'

The complimentary oligonucleotides were used to generate the desired mutation by PCR. Each sample tube contains 5 µL of 10X reaction buffer, 2 µL of plasmid dsDNA template (50 ng), 1 µL of forward primer (125 ng), 1 µL of reverse primer (125 ng), 1 µL of dNTP mix solution and 39.5 µL double-distilled water to a final volume of 50 µL. Following vortexing, the tube was centrifuged briefly and 1 µL of Pfu *Turbo* DNA

polymerase (2.5 U/ $\mu$ L) was added. Thermal cycling was as follows. At the end of the reaction, the tube was immediately placed on ice for 2 min to cool the sample.

First step:	1 cycle	95°C for 30 seconds
Second step:	16 cycles	95°C for 30 seconds
		55°C for 1 minute
		68°C for 7 minutes

Following temperature cycling, the cDNA product was treated with 1  $\mu$ L of the *Dpn* I restriction (10 U/ $\mu$ L) for 1h at 37°C to digest the methylated parental DNA template and to select for the PCR-generated (non-methylated) DNA. After digestion, 1  $\mu$ L of the *Dpn* I-treated DNA was added to 50  $\mu$ L of the super-competent *E. coli* bacteria (provided with the transformation kit) and incubated on ice for 30 min. After the incubation, the reaction was heat-shocked for 45 sec at 42°C and kept on ice for another 2 min. The bacteria were grown in 250  $\mu$ L of SOC medium (980  $\mu$ L SOB (950 mL ddH<sub>2</sub>O; 20 g Bacto Tryptone; 5 g Bacto Yeast Extract; 0.5 g NaCl; 10  $\mu$ L 2 M MgCl<sub>2</sub>; 20  $\mu$ L 1 M glucose) at 37°C, and agitated at 225 rpm for 45 min. The bacteria were then incubated on Luria-Bertani Broth (LB)/Amp<sup>+</sup> agar plates overnight. Positive colonies (those colonies that grew are ampicillin resistant and, thus, contain the plasmid DNA) were selected on the following day.

### **2.2.3 Mini-prep amplification of plasmid DNA.**

Mini-preparation (Mini-prep) was used to isolate small amounts of plasmid DNA from bacteria while limiting contamination by protein and genomic DNA. A single positive colony was picked and cultured in 3 mL of LB (10 g Bacto Tryptone; 5 g Bacto Yeast Extract; 10 g NaCl; taken to 1000 mL H<sub>2</sub>O) (containing 50  $\mu$ g/mL ampicillin). After shaking at 37°C/250 rpm overnight, 1 mL of culture was centrifuged at 12,000g for 30 sec. The cell pellet was fully resuspended in 100  $\mu$ L of ice-cold solution I (50 mM Glucose; 10 mM EDTA, pH 8.0; 25 mM Tris-base, pH 8.0) by vortexing. The cells were then lysed by gently mixing the tube back and forth 10 times with solution II (0.2 N NaOH; 1% sodium dodecyl sulfate (SDS)). Following a 5-min incubation on ice, 150  $\mu$ L

of ice-cold solution III (5 M potassium acetate solution, pH 4.8) was added to the tube and mixed by rapidly inverting the tube 10 times. The sample was centrifuged at 12,000g for 5 min at 4°C and the supernatant was transferred to a new microtube. 450 µL of phenol:chloroform (1:1) was added to the tube to purify the plasmid DNA. After centrifugation at 12,000g for 2 min, the supernatant was transferred to a new tube and 900 µl of room temperature 100% ethanol was used to precipitate the double-strand DNA. The DNA pellet was collected by centrifuging at 12,000g for 10 min and washing with 1mL of ice-cold 85% ethanol. The purified DNA was then re-dissolved in nanopure water containing DNase-free pancreatic RNase (20 U/mL) and incubated for 20 min at room temperature. The plasmid yield was measured by UV-spectrometry at an absorbance of 260 nm. An O.D. ratio of 260 nm: 280 nm was also determined to measure the DNA purity (a ratio of 1.8 or greater was deemed to have minimal protein contamination and could be used for transfection experiments).

#### **2.2.4 Maxi-prep amplification of plasmid DNA.**

The procedure for plasmid DNA maxi-prep is similar to that described above for the mini-prep. Cells were cultured in 5 mL antibiotic-LB broth for 5 h and then transferred into 300-400 mL LB medium to grow for 18 h. Cells were harvested by centrifugation [5000g for 10 min at 4°C] and washes in 100 ml ice-cold 1X STE (0.1 M NaCl; 10 mM, Tris pH 8.0; 1 mM EDTA, pH 8.0). The pellet was lysed with solution I (20 mL), solution II (40 mL) and solution III (20 mL) sequentially (solutions as described for the mini-prep protocol, above), then was centrifuged for 15 min at 5000g at room temperature. The supernatant was filtered through six layers of cheesecloth into a 250 mL centrifuge bottle. 0.6-volume of isopropanol was added and incubated for at least 15 min to precipitate liberated DNA and RNA. Following centrifugation at 5000g for 15 min, the pellet was collected and rinsed with 85% of ethanol. The ethanol was drained and the pellet was re-dissolved in 3 mL of TE buffer (10 mM Tris-base, pH 8.0; 1 mM EDTA, pH8.0). The RNA was precipitated in 4.8 mL ice-cold 5 M LiCl and centrifuge at 9000g for 10 min at 4°C. The plasmid DNA in the supernatant was subsequently precipitated with an equal volume (about 7.8 mL) of isopropanol again and was washed with 85% ethanol. After fully draining the ethanol, 500 µL of TE buffer was added to re-suspend

the DNA pellet. The sample was treated with 5  $\mu\text{L}$  RNase (10 mg/mL) for 30 min at room temperature. Immediately after, 400  $\mu\text{L}$  of 1.6 M NaCl (with 13% (w/v) PEG 800) was mixed with the TE solution and centrifuged at 12,000 rpm for 2 min. Plasmid DNA was purified by two extractions into 500  $\mu\text{L}$  phenol. Chloroform was used to separate phenol from the DNA solution. The concentration of DNA was measured by UV-spectrometry at an absorbance of 260 nm.

### **2.2.5 Transformation of bacterial cells.**

Transformation is a technique routinely used to amplify a gene of interest in molecular biology. The plasmid that contains a specific DNA sequence was inserted into bacterial competent cells (thus ‘transforming’ the bacteria) through artificially induced membrane pores as follows. 1  $\mu\text{L}$  of plasmid DNA was combined with 50  $\mu\text{L}$  competent DH-5 $\alpha$  *E. coli* cells in each transformation reaction. After 30 min of incubation on ice, the reaction tube was then heat-shocked at 42°C for 45-60 sec. In order to allow the cell membrane to heal, a 2-min incubation on ice was needed. Then cells were cultured in 250  $\mu\text{L}$  of SOC medium at 37°C for 45 min with shaking at 225 rpm. 30  $\mu\text{L}$  of the cell suspension was spread on an agar plate (containing the appropriate antibiotic) and grown in an incubator (37°C) overnight. Individual colonies were collected and subjected to PCR to confirm the presence of the plasmid.

### **2.2.6 Transient transfection of mammalian cultures.**

For this part of the project, plasmid DNA was transferred into mammalian cells, e.g. N2a and HT-22 cells. The protein was then allowed to be expressed for 24 hours (hence, ‘transient’ transfection).  $3 \times 10^6$  cells were plated in 100 mm cell culture dishes. DNA and Lipofectamine 2000 reagent were diluted to a predetermined concentration in separate microcentrifuge tubes (for a final ratio of DNA:Lipofectamine 2000 of 1.5  $\mu\text{g}$ :2.5  $\mu\text{L}$ ) with serum-free OPTI-MEM medium and incubated for 5 min. The two solutions were then combined at room temperature for 20 min to allow for the formation of DNA-Lipofectamine 2000 complex. The mixture was added directly into each cell culture and the culture medium was replaced 4 hours after the transfection to avoid any toxicity associated with the Lipofectamine 2000 reagent.



### 2.2.7 Immunoblot/Western Blot assay.

Immunoblot/Western Blot is a powerful technique for examining a protein of interest. Equal amounts of denatured protein from total cell lysates were resolved on an SDS-polyacrylamide gel (SDS-PAGE: the proteins migrate based on their molecular weight). The resolved proteins were probed using specific antibodies the target the protein and secondary antibodies (*i.e.* antibodies that recognize the specific primary antibody and that have been conjugated with horseradish peroxidase to allow for a chemiluminescent reaction) were used to reveal the protein band on photographic film.

Briefly, transfected cells were harvested and washed with 1X PBS. Following centrifugation at 1000g for 5 min at room temperature, the supernatant was removed and the cell pellet was lysed with Lysis buffer (1% Triton-X 100; 20 mM Tris, pH 7.5; 10% glycerol; 1 mM EDTA) containing 100X protease inhibitor cocktail. The lysate was vortexed and incubated on ice for 30 min; then centrifuged at 16,000g at 4 °C for 20 min. The supernatant was retained as it contained the soluble protein. The protein concentration was determined by BCA protein assay kit. Each sample was denatured by heating to 95°C for 5 min with 4X Laemmli Buffer (8% SDS; 40% glycerol; 10% mercaptoethanol; 0.02% bromophenol blue; 0.25 M tris-HCL, pH 6.8).

The Mini-PROTEAN Tetra electrophoresis system and Mini Trans-Blot Cell system were both used (with comparable results) for the electrophoresis and transfer. A 10% resolving gel (4mL ddH<sub>2</sub>O; 2.50 mL Buffer A (18.45 g Tris-HCL; 77 g Tris-base; 2 g SDS; 500 mL H<sub>2</sub>O; pH 8.8); 3.33 mL 30% acrylamide; 100 µL 10% SDS; 50 µL 10% APS; 10 µL TEMED) and 4% stacking gel (3 mL ddH<sub>2</sub>O; 1.25 mL Buffer C (30g Tris-base 2 g SDS; 500 mL H<sub>2</sub>O, pH 6.8); 0.67 mL 30% acrylamide; 50 µL 10% SDS; 25 µL 10% APS; 5 µL TEMED) were prepared. Running buffer was made by mixing 3.03 g Tris-base, 14.4 g glycine and 10 g SDS in a final volume of 1000 mL H<sub>2</sub>O. The proteins were resolved by SDS-PAGE electrophoresis (at a constant voltage of 110V for 1.5 to 2 h). Proteins were then transferred onto a 0.22 µm nitrocellulose membrane at a constant current of 230 mA for 1.5 h in ice-cold running buffer (3.03 g Tris-base; 14.4 g glycine; 10 g SDS; taken to 1000 mL with H<sub>2</sub>O).

Membranes were blocked with 5% (m/v) skimmed milk in TBS buffer (3 g Tris-

base; 8 g NaCl; taken to 1000 mL with H<sub>2</sub>O) for 1h at room temperature and then incubated with a 1:1000 dilution of the antibody in TBS-Tween<sup>®</sup> 20-0.5% bovine serum albumin (BSA) overnight at 4°C. The membranes were washed three times for 10 min with TBST and then incubated with a 1:2000 dilution of the secondary antibody in 5% milk-TBST for another hour at room temperature. Following three washes with TBST, the membranes were processed by enhanced chemiluminescence (ECL) and exposed to a film. All of the washing and incubation steps were carried out on a shaker.

### **2.2.8 Immunoprecipitation.**

Immunoprecipitation (IP) is a technique used to investigate whether two proteins physically associate, and/or to confirm the biochemical characteristics, posttranslational modifications and expression levels of a given protein. IP involves the targeting of a protein by a specific antibody and then precipitation of the immune complex with sepharose beads on which have been attached either protein-G or protein-A (bacterial derived proteins that bind the Fc portion of mammalian IgG antibodies).

Cells were harvested and lysed as usual (see 2.2.7). For each IP sample, 300-500 µg of protein was prepared. Non-specific mouse IgG at a ratio of 1:100 (antibody: protein) and 30-50 µL of sepharose-A/G were added to the lysate for pre-clearing of the protein extract at 4°C for 1-2 h (preclearing removes any non-specific reaction between antibody, sepharose and protein). 5-10 µg of antibody was incubated overnight (4°C) with the pre-cleared extract, following which 50 µL of washed protein-A/G beads were added to the sample. The samples were then incubated (with shaking for 1 h at 4°C) and then the beads were pelleted by centrifugation at 9000g for 5 min and then resuspended in lysis buffer. This was repeated three times. After the last wash, the beads were boiled at 95°C for 5 min with 25 µL of 1X loading buffer.

### **2.2.9 MTT conversion assay.**

MTT conversion was used as an indicator of mitochondrial function/cell viability. 3-(4,5-dimethylthiazol-2-yl)-2,5-diphenyltetrazolium bromide (MTT) stock (5 mg/mL) was prepared by dissolving MTT in PBS and filtering this solution through a 0.22 µm filter to remove the minute traces of undissolved MTT. The working solution (0.5

mg/mL) was made by mixing 1 volume of stock MTT solution with 9 volumes of DMEM media containing 1% FBS.

Cells were first seeded in a 96-well plate and grown overnight in 5% CO<sub>2</sub> incubator. After treatment of cells for 24 h, experimental media was carefully removed and 50 µL of the MTT working solution was added to each well. The cells were then incubated in a 5% CO<sub>2</sub> incubator at 37°C for 4 h. 100 µl of DMSO was added and thoroughly mixed to dissolve the purple formazan crystals generated by conversion of the MTT substrate. The plates were immediately read at an absorbance of 570 nm. These values were used to estimate cell viability. The average OD values of control group (vector transfected cells) were set to 100% of cell viability.

#### **2.2.10 MAO-A activity assay.**

MAO-A catalytic activity was assessed using a radioenzymatic protocol. The enzymatic rate of conversion of MAO-A to aldehydes is estimated using [<sup>14</sup>C]-labeled serotonin (5-HT) as the substrate and a potassium phosphate reaction buffer (181.6 ml 1M K<sub>2</sub>HPO<sub>4</sub>, 18.4 ml 1M KH<sub>2</sub>PO<sub>4</sub>, taken to 1000 ml with H<sub>2</sub>O, pH 7.85). The buffer must be oxygenated for 30 min at room temperature before use [127]. 100 µg protein homogenates (in 50 µl oxygen-saturated potassium buffer) were incubated with 50 µl serotonin (0.25 mM 5-HT and 25 nCi of [<sup>14</sup>C]-5-HT) at 37 °C for 10 min. The reaction was terminated by acidification (10 µl of 3M HCL). The radiolabeled aldehyde metabolite was extracted into 1 ml of H<sub>2</sub>O-saturated ethyl acetate:toluene (1:1) solution. The sample was mixed by vortexing and centrifuging at 14,000g for 30 seconds. After centrifugation, 700 µl of top layer (organic phase) was transferred to a liquid scintillation vial containing 4 ml of scintillation cocktail. The amount of radioactive metabolite, estimated as dpm (disintegrations per minute), was measured on a Beckman counter. The blank control was made by mixing protein with substrate, but the reaction was quenched by acidification before it could take place. The standard was 50 µl of radiolabeled serotonin substrate. The activity of MAO-A was calculated based on the formula:

$$\text{MAO-A activity (nmol/mg protein/min)} = \frac{\text{Dpm sample - Dpm Blank}}{\text{Dpm standard}} \times \underset{\substack{\text{time} \\ \text{coefficient}}}{\downarrow} 6 \times \underset{\substack{\text{partition} \\ \text{coefficient}}}{\downarrow} 1.15$$

$$\frac{700\mu\text{l} / 1000\mu\text{l} \times \text{Protein concentration} \times 50\mu\text{L}}{\substack{\uparrow \\ \text{extraction} \\ \text{ratio}} \quad \substack{\uparrow \\ \text{protein amount}}}$$

Ca<sup>2+</sup>-sensitive MAO-A activity was determined by pre-incubation of the homogenates with 1 mM Ca<sup>2+</sup> for 20 min at room temperature prior to the reaction [128, 129].

### 2.2.11 Brain regional dissection.

Brains were rapidly removed from the test mice and were placed on a cutting platform, which was kept cold on dry ice. After removing the cerebellum from the brainstem, the blade was carefully inserted into the central sulcus and used to separate the brain in two (sagittally). Although various regions were collected (hippocampus, striatum), only the cortex and cerebellum were used for the current project. All samples were flash-frozen and stored at -70°C until assayed.

### 2.2.12 High-pressure liquid chromatography (HPLC).

HPLC determinations were performed using a Bioanalytical Systems (West Lafayette, IN, USA) LC-4B amperometric detector and a Hewlett-Packard (Palo Alto, CA, U.S.A.) 3392A integrator. The compounds of interest were measured using a glassy carbon electrode set at 0.75 V versus an Ag/AgCl reference electrode. The flow rate was 1 ml/min through a C18 column (4.6 mm x 250 mm; 5 µm particle size, Applied Science Labs, Avondale, PA, USA) coupled to a precolumn. The mobile phase consisted of NaH<sub>2</sub>PO<sub>4</sub> (55 mM), sodium octyl sulfate (0.85 mM), disodium EDTA (0.37 mM) and acetonitrile (9%) and was filtered, degassed, and adjusted to pH 3.0. The concentrations of analytes were determined by comparing peak height ratios to those of a set of authentic standards processed in parallel [130]. These analyses were done in collaboration with Dr. G.B. Baker (Neurochemical Research Unit, Psychiatry, University of Alberta).

### **2.2.13 Immunohistochemistry.**

Sagittally separated brains were fixed and sliced with the help of Tuo Zhao (another M.Sc. student in our laboratory). Animals were first perfused with 0.1 M PBS (pH 7.4) and then brains were post-fixed in paraformaldehyde (4%: 24 h). The brains were then transferred to cryoprotectant (30% glycerol/0.1M phosphate buffer, 48 h), then snap-frozen and stored at -70°C until sectioned (30 µm, coronally). The sections were then stored (25% glycerol; 25% ethylene glycol; 0.1M PBS) at 4°C until processed.

3,3'-Diaminobenzidine (DAB)-immunohistochemistry was performed on free-floating sections that had been rinsed in 0.01 PBS, treated with 0.2% H<sub>2</sub>O<sub>2</sub> in 0.1M PBS (30 min) and blocked in 5% normal serum in PBS containing 0.2% Triton (PBS-TX) (1.5 h). Sections were then incubated (4°C) for 72 h with the polyclonal H-70 MAO-A antibody (1:100) in 5% normal serum-PBS-TX, and then incubated with biotinylated goat anti-rabbit (BA-1000, Vector Laboratories Canada) (1:250, 1.5 hours) and processed by the ABC-DAB method. All steps were followed by washes in PBS (3x20 min). The sections were also processed for thionin/Nissl staining. Sections were mounted on gelatin-coated slides, dehydrated in ascending alcohols, cleared with xylene, and coverslipped with Permount for visualization using a Olympus BX51 fluorescence microscope.

### **2.1.14 Forced-swim test.**

The forced swim test, originally developed by Porsolt and colleagues to screen for antidepressant drugs [131], is a behavioural test designed to measure 'despair'. After the drug treatment, animals are placed in a tank of water that does not allow them to touch the bottom. They are tested for an extended period of time and observed for their mobility, *i.e.* making 'swimming' movements to keep their head above the water. The time that the rodents spend 'swimming' is recorded. The time that animals are immobile can be decreased by antidepressants and, hence, was thought to be a good assay for antidepressant drugs [131]. For my studies, a glass cylinder (46 cm tall x 20 cm in diameter) was used. The cylinder contained 30-cm deep water and was maintained at 22°C. Clorgyline (CLG: 1 mg/kg, *i.p.*) was administered acutely (2 h before the testing period) to 6-month old wildtype and PS-1(M146V) mice. This dose-regimen of CLG was

chosen as it does not affect either immobility time in the Forced-Swim Test [132] or ambulatory behaviour [133] in wildtype mice, but it does affect the tissue content of monoaminergic neurotransmitters [133]. Mice were timed concurrently by four independent observers. The water was changed between test runs.

#### **2.1.15 Statistical analyses.**

Data were analyzed by unpaired t-test (for comparing between two means) or one-way analysis of variance (ANOVA) (for comparing between more than two means). t-test statistics are reported as, for example, [ $t=3.168$ ,  $df=8$ ,  $P=0.0132$ ], where ‘t’ is the test value, ‘df’ are the degrees of freedom, and ‘P’ is the corresponding probability. F-test statistics are reported as, for example, [ $F_{(3,19)}=0.7126$ ,  $P=0.5586$ ], where ‘F’ is the test value, ‘(3,19)’ are the degrees of freedom between groups (number of groups minus ‘1’, so 4 groups - 1 = 3) and within samples (total number of samples minus ‘1’, so 20 samples - 1 = 19), and ‘P’ is the corresponding probability. A P value (probability, i.e., a number expressing the chances that a specific event will occur) of less than 0.05 was set as statistically significant (e.g. there is less than a 5% (0.05) chance that an effect is due strictly to random chance). *Post-hoc* analysis relied on the Bonferroni’s Multiple Comparison Test (PRISM v3.0; GraphPad Software Inc., San Diego, CA, USA). The Bonferroni’s Multiple Comparison Test was used as it is a very stringent statistical test and any conclusions based on this test are certainly reliable. All data were expressed as means  $\pm$  SEM (unless otherwise indicated). Symbols were used according to convention, i.e. \*:  $P<0.05$ , \*\*:  $P<0.01$ , \*\*\*:  $P<0.001$ .

### 3. Results

#### Part I: Effects of PS-1 (M146V) variant on MAO-A function in mice.

##### 3.1 MAO-A activity is affected in the PS-1 (M146V) knock-in mice.

A previous M.Sc. student in our research group, Geraldine Gabriel, originally tested the effects of four PS-1 mutants (D257A, Y115H,  $\Delta$ Ex9 and M146V) on MAO-A function. She found that the endogenous MAO-A activity in HT-22 cells was altered differently by these PS-1 constructs [134]. The PS-1(M146V) protein did not alter HT-22 MAO-A activity compared to the vector-transfected control, but did have an effect on increase calcium ( $\text{Ca}^{2+}$ )-sensitive MAO-A activity. There is evidence that a significant disruption of  $\text{Ca}^{2+}$  homeostasis can be observed in PS-1 (M146V) mice [105]. Since PS-1 (M146V) is clearly associated with familial AD and the animal model also is available commercially, I chose to start my studies by examining  $\text{Ca}^{2+}$ -sensitivity of MAO-A in the PS-1(M146V) mouse at two different ages. In order to ensure that any changes would be *independent* of any change in A $\beta$  burden and, thus, only due to the expression of the mutant PS-1 protein, 3- and 6-month old were chosen for the following experiments.

Cortical and cerebellar tissues from 3-month and 6-month-old wildtype and PS-1(M146V) mice were tested for both basal and  $\text{Ca}^{2+}$ -sensitive MAO-A activity. In cortical homogenates, activity did not change in either wildtype or 3-month PS-1(M146V) mice. However,  $\text{Ca}^{2+}$ -sensitive MAO-A activity was increased in 6-month PS-1(M146V) mice by approximately 25% (Figure 3.1) [ $F_{(3,19)}=6.286$ ,  $P=0.0051$ ]. In cerebellar homogenates, neither basal or  $\text{Ca}^{2+}$ -sensitive MAO-A activity was affected (Figure 3.1) [ $F_{(3,19)}=0.7126$ ,  $P=0.5586$ ]. Therefore, 6-month old mice were used for the remainder of the experiments.

MAO-A protein level was also analyzed by immuno- (Western) blot (Figure 3.2). The protein amount from cortical extracts in PS-1(M146V) 6-month old mice was increased approximately 50%, as assessed by ImageJ 1.32j densitometry (<http://rsb.info.nih.gov/ij/>) [ $t=3.168$ ,  $df=8$ ,  $P=0.0132$ ]. Therefore, two conclusions can be immediately made: first, the PS-1(M146V) protein appears to affect MAO-A activity *in vivo*, and, second, the mismatch between MAO-A protein induction (~50%) and MAO-A

catalytic activity (no change in basal activity) suggests a potential post-translational regulation of MAO-A function.

### **3.2 Nissl/thionin staining in wildtype and PS-1 (M146V) mouse sensorimotor cortex.**

Since MAO-A activity was found to be different in the cortex between wildtype and PS-1(M146V) mice, tissue sections were taken from 6-month old mice cortex for determining protein expression by immunohistochemistry. Nissl staining is used to reveal "Nissl bodies" (rough endoplasmic reticulum) which are abundant in neurons; this technique is often used to examine and reveal specific patterns of cytoarchitecture in the brain. Examination (40X and 100X) of wildtype cortex reveals a distinct architecture of 6 layers (Figure 3.3B,C). In contrast, cells from the same region in the PS-1(M146V) mouse cortex appear to be disorganized and the laminar boundaries are lost (Figure 3.3E,F). These cortical sections were also used for DAB-MAO-A immunohistochemistry (Figure 3.3A,D). While MAO-A immunodetection was apparently concentrated in layer V of wildtype cortex, an abnormal distribution of the MAO-A protein was observed in PS-1(M146V) cortex. It is clear that the presence of the PS-1(M146V) transgene affects cortical structure and that this also has an effect on MAO-A distribution (and perhaps function). MAO-A function in these animals was tested in the next section.

### **3.3 The MAO-A inhibitor clorgyline (CLG) exerts behavioural changes in PS-1(M146V) mice.**

The forced-swim test was used to examine non-cognitive behaviours in the PS-1(M146V) mice. It is a test of behavioural despair (akin to depression in humans). Treatments [saline or CLG (1 mg/kg), n=6-9] were administered 2 hr prior to a 6-min test swim (includes a pre-exposure period of 2 minutes followed by a 4-minute test session immediately thereafter). Saline solution was given to the control animal group as vehicle treatment. Mice were placed in the water and the time that they spent 'swimming' was recorded. Figure 3.4 suggests that wildtype mice (black bars) perform the same regardless of treatment. In contrast, CLG decreased the time that PS-1(M146V) mice (grey bars) spent swimming [ $F_{(3,24)}=3.425$ ,  $P=0.0359$ ].



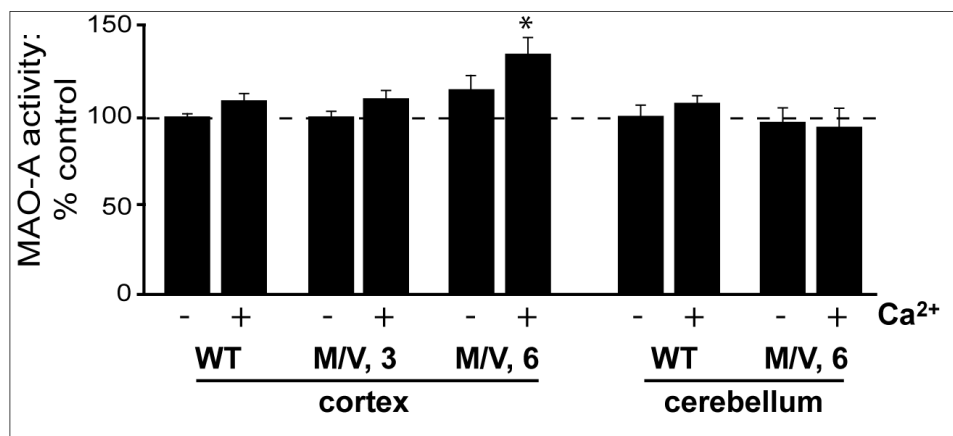


**Figure 3.1: MAO-A activity with and without Ca<sup>2+</sup> in wildtype and PS-1 (M146V) mice.** Cortical extracts from 3- and 6-month old mice expressing the PS-1(M146V) protein were assayed for MAO-A activity. The Ca<sup>2+</sup>-sensitive activity was only increased in cortex of 6-month old PS-1(M146V) mice (M/V, 6). The effect of PS-1(M146V) appears to be age-dependent as well as region-dependent as there was no obvious effect of the transgene on MAO-A activity in cerebellar extracts. \*:  $P < 0.05$  versus Ca<sup>2+</sup>-sensitive MAO-A activity in WT cortical extracts (mean $\pm$ SEM, n=5-6).

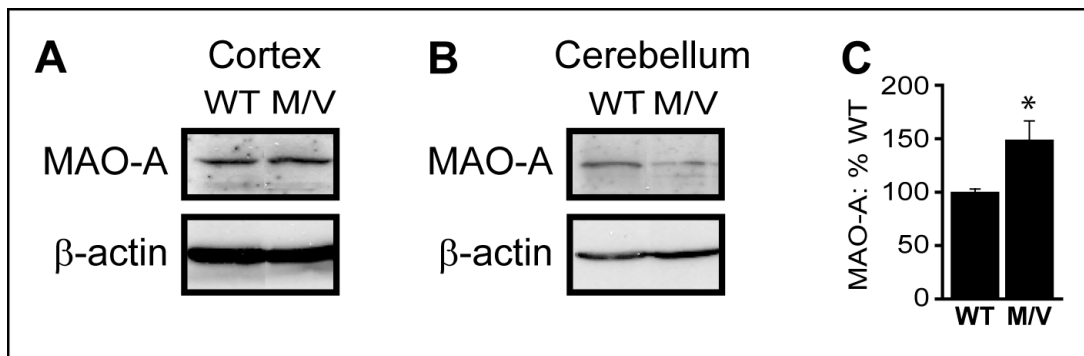


**Figure 3.2: MAO-A expression in cortex and cerebellum of PS-1(M146V) mice.** Endogenous MAO-A protein in cortex (A) and cerebellum (B) region in 6-month old wildtype (WT) and PS-1(M146V) (M/V) mice was detected using Western blot analysis based on the MAO-A H-70 antibody. (C) Densitometry reveals that cortical MAO-A expression increases by approximately 50% in PS-1(M146V) mice. \*:  $P < 0.05$  versus wildtype levels (n=5).

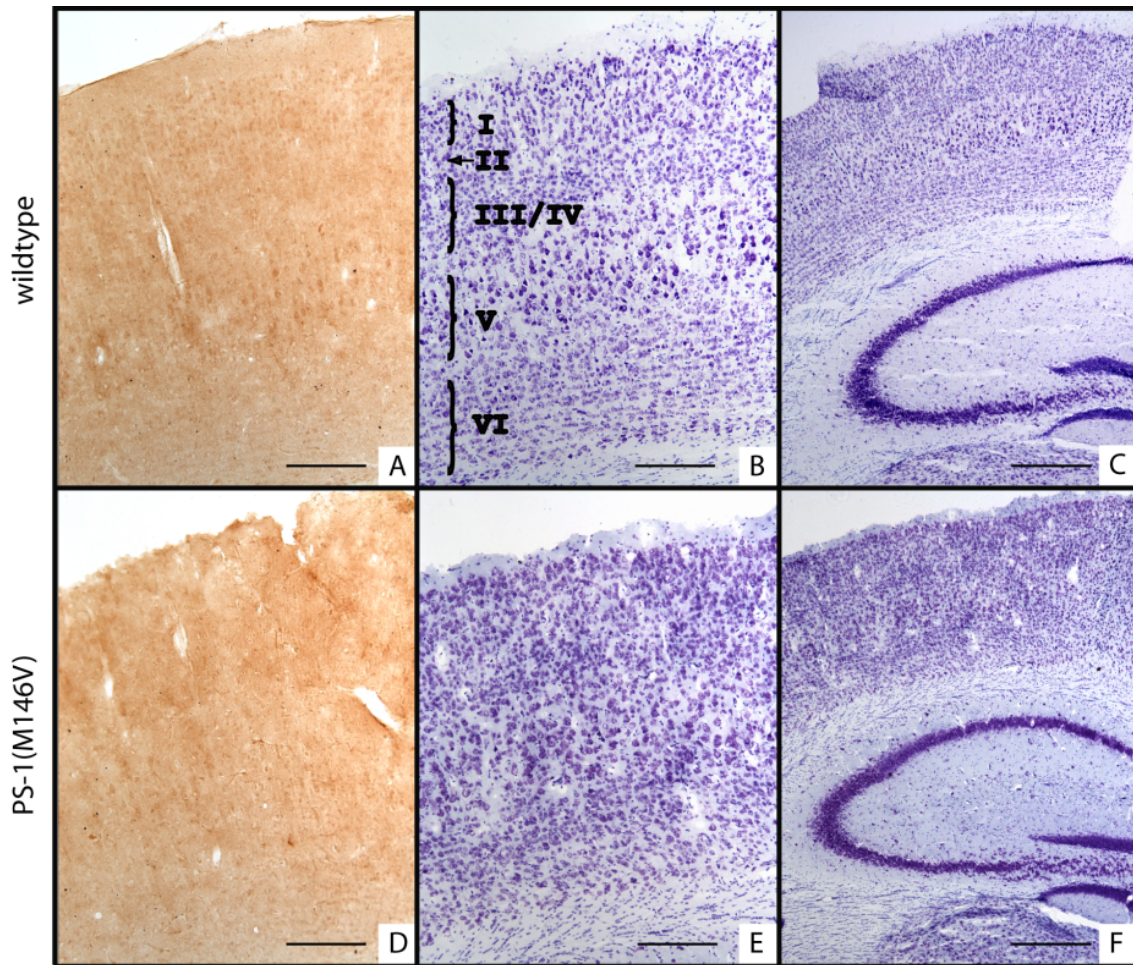


**Figure 3.3: MAO-A distribution and Nissl staining in wildtype and PS-1(M146V) mice sensorimotor cortex.** Coronal cortical sections of (A-C) wildtype and (D-F) PS-1(M146V) mice were used for Nissl staining (B, C, E, F) and DAB-MAO-A immunohistochemistry (A, D). Scale bars=125  $\mu\text{m}$  (A, B, D, E; 100X magnification) and 500  $\mu\text{m}$  (C, F: 40X magnification).

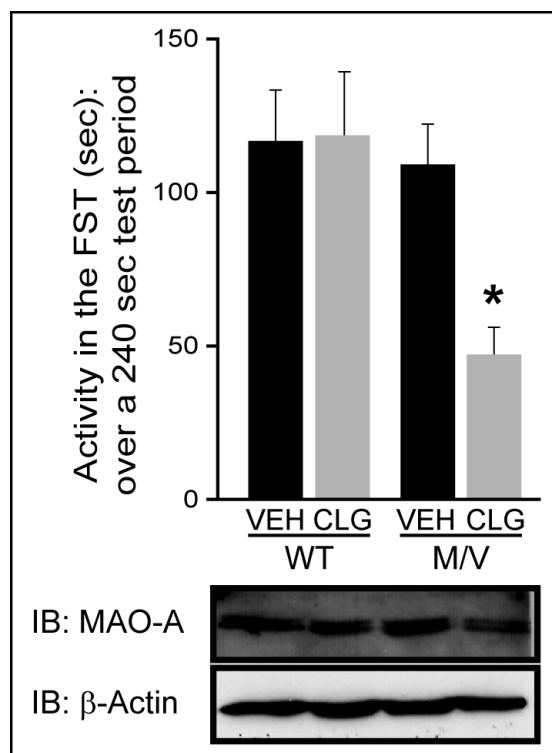


**Figure 3.4: MAO-A-sensitive non-cognitive behaviour is revealed in the PS-1(M146V) mice.** 6-month-old PS-1(M146V) (M/V) mice and wildtype (WT) littermates were treated with either the saline vehicle (VEH) or the selective MAO-A inhibitor clorgyline (CLG; 1 mg/kg, i.p., 2 h). Their ‘activity’, i.e. the time that they spent swimming during the 240 sec test period of the forced-swim test (FST), was measured. Western blot/Immunoblot (IB) demonstrates MAO-A protein expression in corresponding cortical extracts.  $\beta$ -Actin is used to demonstrate equal protein loading across lanes. \*:  $P < 0.05$  versus vehicle-treated PS-1(M146V) mice (mean $\pm$ SEM, n=6-8).

### 3.4 Levels of selected monoamine and acid metabolites in the cortex and cerebellum of wildtype and PS-1(M146V) mice.

Figure 3.1 suggests that expression of the PS-1(M146V) protein affects MAO-A function in a region-specific manner. As MAO-A is known to degrade monoamine such as 5-HT, dopamine (DA) and norepinephrine (NE), it was important to determine whether these monoamines were affected in the PS-1(M146V) mouse. The cortex and cerebellum from the 6-month wildtype and PS-1(M146V) mice that had been subjected to the forced-swim test were immediately sacrificed and used for neurochemical analyses using high-pressure liquid chromatography. In addition to the monoamines listed above, acid metabolites of 5-HT, i.e. 5-HIAA (5-hydroxyindolacetic acid), and DA, i.e. DOPAC (3,4-dihydroxyphenylacetic acid) and HVA (homovanillic acid), were also measured. This work was done in collaboration with Dr. G.B. Baker (Neurochemical Research Unit, Psychiatry, University of Alberta).

The statistics for 5-HT and 5-HIAA levels in **cortical** extracts were as follows: 5-HT [F(3,36)=12.99, P<0.0001] and 5-HIAA [F(3,39)=18.95, P<0.0001] (Figure 3.5). For 5-HT and 5-HIAA levels in **cerebellar** extracts, the statistics were as follows: 5-HT [F(3,36)=9.331, P=0.0001]; 5-HIAA [F(3,36)=2.390, P=0.0864] (Figure 3.5). The statistics for DA, NA and metabolite levels in **cortical** extracts were as follows: DA [F(3,30)=2.266, P=0.1035], DOPAC [F(3,33)=5.540, P=0.0041], HVA [F(3,37)=6.528, P=0.0013], NA [F(3,38)=5.017, P=0.0054] (Figure 3.6). For DA, NA and metabolite levels in **cerebellar** extracts, the statistics were as follows: DA [F(3,34)=8.963, P=0.0002], DOPAC [F(3,32)=0.664, P=0.5929], HVA [F(3,34)=2.810, P=0.0557], NA [F(3,30)=34.63, P<0.0001] (Figure 3.6). Post hoc analyses revealed that the PS-1(M146V) knock-in exerted changes in cortical amine and metabolite levels that, in general, resemble characteristic MAO inhibition, *i.e.* amine levels increase while corresponding metabolite (DOPAC and 5-HIAA) levels decrease (Figs. 3.5 & 3.6). Similarly, treatment with CLG resulted in characteristic changes in catecholamine levels, but, surprisingly, did not significantly affect the levels of 5-HT or 5-HIAA. This pattern of change was inconsistent with the changes observed in cerebellar extracts, wherein the PS-1(M146V) variant tended to generally decrease the levels of these amines and metabolites, whereas

treatment with CLG only resulted in the accumulation of 5-HT and NA. These data suggest that PS-1(M146V) functionally inhibits cortical MAO-A and that acute treatment with CLG elicits region-specific (and potentially uncharacteristic) effects on monoaminergic metabolism in this model.

### **3.5 Clorgyline (CLG) is more potent in PS-1 (M146V) mice than in wildtype mice.**

Cortical and cerebellar homogenates from 6-month wildtype and PS-1(M146V) mice were tested *ex vivo* for MAO-A activity to confirm that they had received the treatments according to Figures 3.4, 3.5 & 3.6.

With wildtype cortical homogenates it was observed that the MAO-A activity decreased by approximately 50% (compared to the vehicle-treated group) after treatment with CLG [ $F_{(3,18)}=20.02$ ,  $P<0.0001$ ]. Unexpectedly, MAO-A activity was almost completely inhibited in the CLG-treated PS-1(M146V) mice (Figure 3.7A). In cerebellum, the CLG had a very similar effect as determined for the cortex (Figure 3.7B) [ $F_{(3,16)}=36.87$ ,  $P<0.0001$ ]. Thus, the potency of the MAO-A-selective inhibitor CLG is increased by the PS-1(M146V) protein *in vivo*.

### **3.6 CLG dose-response curves in wildtype and PS-1(M146V) mice.**

CLG dose-response curves (n=4) were generated using the cortical extracts from vehicle-treated wildtype and PS-1(M146V) mice in Section 3.5 above. The cortical extracts were pre-incubated with CLG (final concentration ranging from  $10^{-8}$  to  $10^2$   $\mu$ M) for 20 min at room temperature. CLG dose-response curves using cortical extracts from WT [ $R^2=0.9987$ ] mice and PS-1(M146V) [ $R^2=0.9988$ ] mice revealed logIC<sub>50</sub> values ( $\mu$ M) of -2.39 ( $\pm 0.073$ ) and -1.95 ( $\pm 0.045$ ), respectively, which, although statistically significant [ $t=11.44$ ,  $df=6$ ,  $P<0.0001$ ], is not a pharmacologically substantial shift in the response curve (Fig. 3.8). The respective Hill coefficients were -0.827 ( $\pm 0.084$ ) and -1.209 ( $\pm 0.187$ ) [ $t=3.734$ ,  $df=6$ ,  $P=0.0097$ ]. This difference suggests a change in cooperativity.

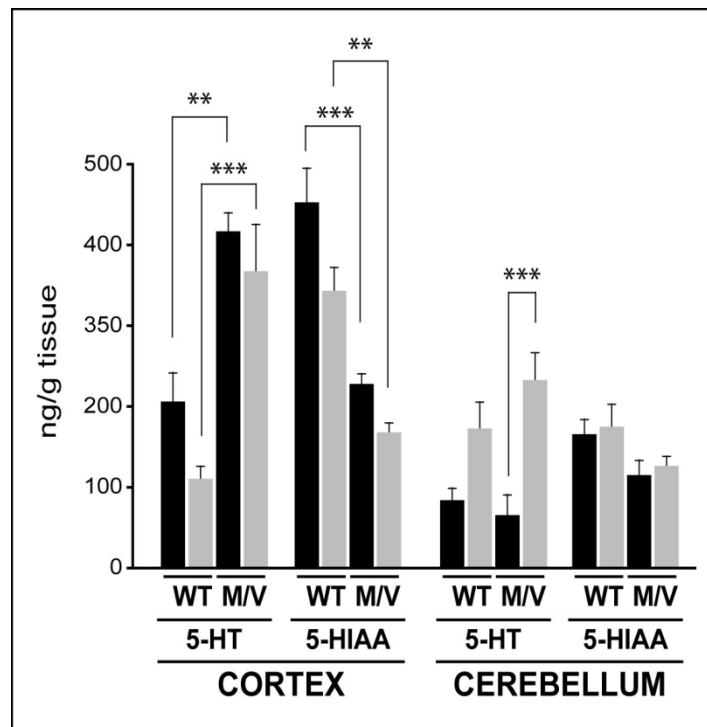


**Figure 3.5: Cortical and cerebellar levels of indoleamines.** Serotonin (5-HT) levels and its MAO-A-mediated acid metabolite 5-HIAA were measured by HPLC in cortical (left) and cerebellar (right) extracts from both wildtype (WT) and PS-1(M146V) (M/V) mice treated with either the saline vehicle (black bars) or the MAO-A inhibitor clorgyline (grey bars: 1 mg/kg, 2 h, grey bars). \*\*:  $P < 0.01$ , \*\*\*:  $P < 0.001$ , between indicated groups (mean $\pm$ SEM, n=8-13).

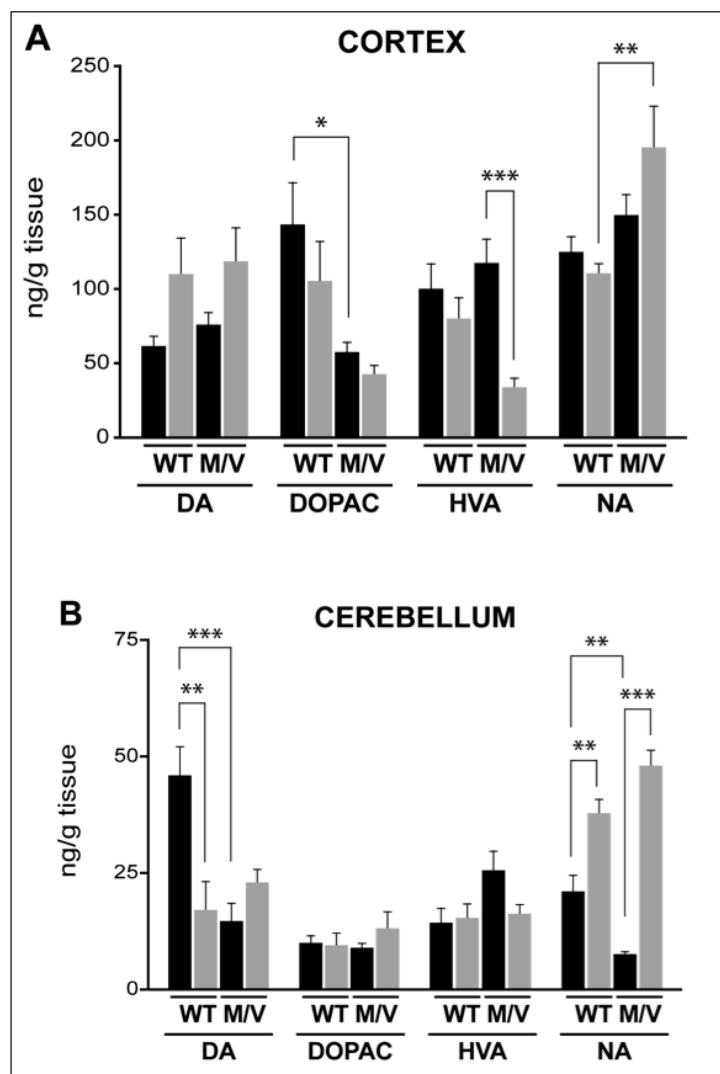


**Figure 3.6: Cortical and cerebellar levels of catecholamines.** Levels of DA and its two acid metabolites (DOPAC & HVA) as well as levels of NA were examined in cortical and cerebellar tissue of 6-month old wildtype and PS-1(M146V) mice. Both of the groups of mice were injected with saline vehicle (black bars) or 1 mg/kg of clorgyline (grey bars) for two hours at which point they were sacrificed for neurochemical analyses. \*:  $P < 0.05$ ; \*\*:  $P < 0.01$ , \*\*\*:  $P < 0.001$ , between indicated groups (mean $\pm$ SEM, n=8-13).



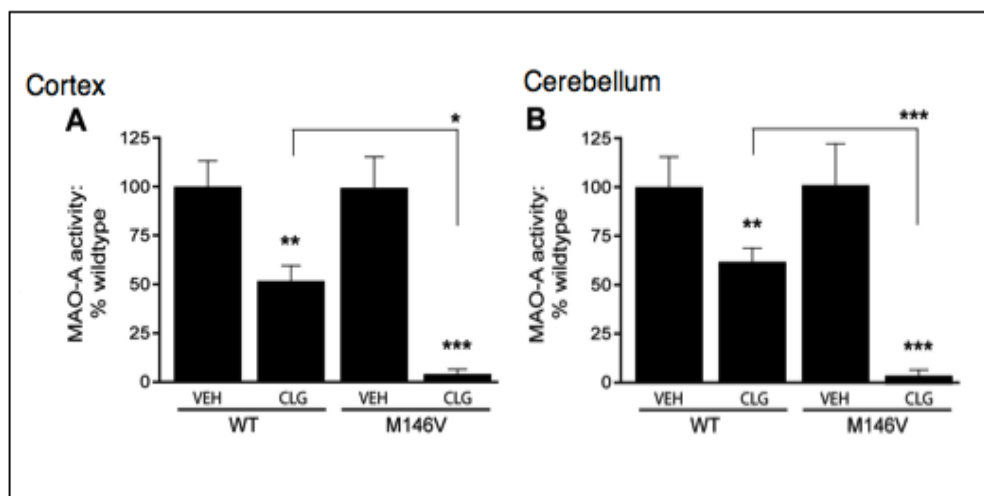


**Figure 3.7: The potency of CLG is increased by the PS-1(M146V) protein *in vivo*.** The extent of inhibition of MAO-A activity was tested in (A) cortical and (B) cerebellar tissue extracts from wildtype (WT) or PS-1(M146V) mice used for behavioural and neurochemical analyses in previous experiments. CLG is more potent in both the cortex and cerebellum of PS-1(M146V) mice. \*:  $P < 0.05$ ; \*\*:  $P < 0.01$ , \*\*\*:  $P < 0.001$ , versus the respective vehicle (VEH)-treated group or between indicated groups (mean $\pm$ SEM, n=8-13).

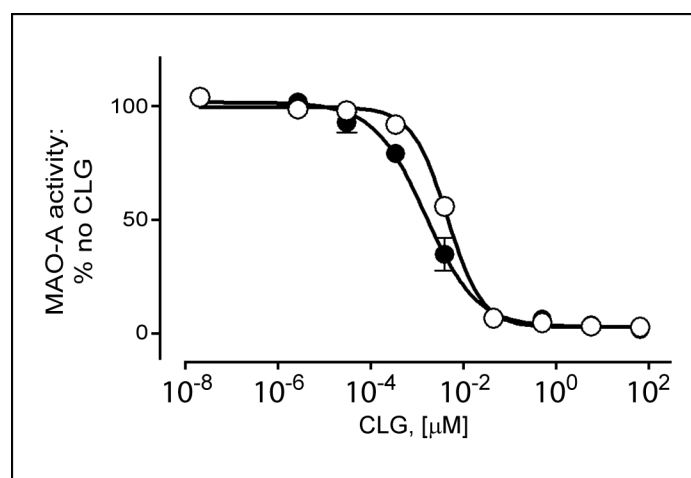


**Figure 3.8: CLG dose-response curve in vehicle-treated wildtype and PS-1(M146V) cortical homogenates.** These curves were generated using cortical tissue homogenates from wildtype (filled circles) and PS-1(M146V) (open circles) animals. Individual homogenates were incubated with increasing concentrations of CLG (in  $\mu\text{M}$ ) for 20 min at room temperature before the assay. Data points represent mean  $\pm$  SEM (n=4).

## **Part II: Direct interaction between PS-1 and MAO-A proteins in animal and cell extracts.**

Results from G.G. Gabriel's M.Sc. thesis work [134] demonstrated that certain AD-related PS-1 variants could affect MAO-A protein and function. The current thesis reveals that  $\text{Ca}^{2+}$  can alter MAO-A function in an age-dependent manner in the PS-1(M146V) mouse cortex (Figure 3.1) and that MAO-A protein induction (Figure 3.2) does not necessarily result in an increase in MAO-A catalytic activity, thus suggesting a post-translational event might be involved. Clearly, the PS-1(M146V) mice respond differently to MAO-A inhibition during behavioural test (Figure 3.4) and their monoaminergic tone is also affected (Figure 3.5 & 3.6). The change in the potency of CLG in the PS-1(M146V) mouse suggests that the MAO-A protein in these mice is somehow altered or influenced (Figure 3.7 & 3.8). CLG dose-response curves revealed differences in the respective Hill coefficients which suggest a change in cooperativity and a change in conformation or access by the substrate to the catalytic pocket.

At this point, I chose to re-direct my studies to cell culture-based approaches so that I could investigate the effect of PS-1(M146V) on MAO-A more closely.

### **3.8 PS-1(M146V) affects $\text{Ca}^{2+}$ -sensitive MAO-A activity in HT-22 cells.**

Therefore, the next series of experiments were focused on *in vitro assays*. Before starting the test using cell cultures, I selected four cell lines to examine their overexpression ability as well as endogenous MAO-A/PS-1 level. Among the four different cell lines, which are HT-22, HEK, N2a and PC12, HT-22 cells have a high basal MAO-A activity while N2a and HEK cells are almost functionally null. As such, I chose to use HT-22 cells to examine the effects of drug or overexpressed PS-1 mutant on *endogenous* MAO-A activity and, when necessary, N2a cells for the study of protein interaction using *overexpressed* MAO-A protein(s).

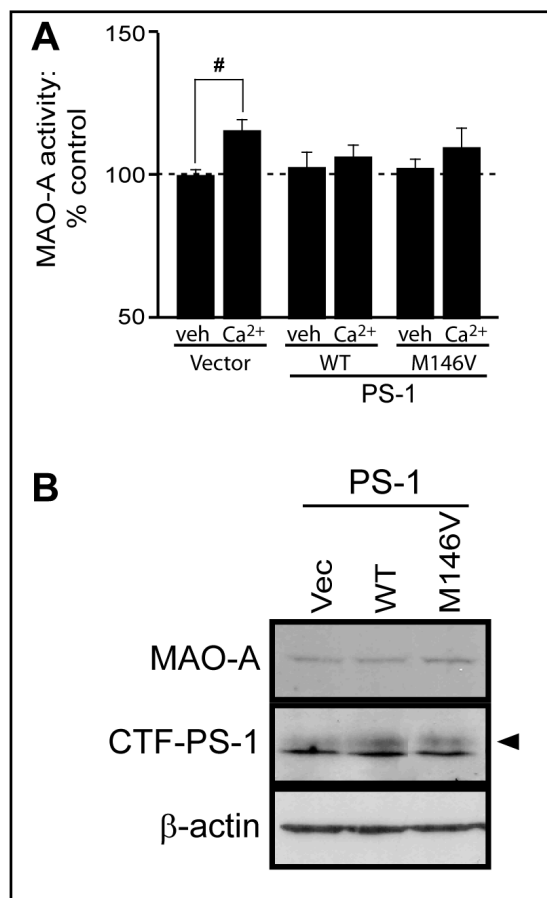


**Figure 3.9: Overexpression of PS-1 wildtype and PS-1(M146V) affects Ca<sup>2+</sup>-MAO-A activity in HT-22 cells.** (A) Basal (veh: 0 mM Ca<sup>2+</sup>) level of MAO-A activity is not significantly different between vector-, PS-1 wildtype- and PS-1(M146V)-transfected cells. 1 mM Ca<sup>2+</sup> slightly increased (about 20%) MAO-A activity in vector-transfected cells, but this was reduced significantly in PS-1 wildtype- and PS-1(M146V)-transfected cells. (B) The expression of PS1 wildtype as well as M146V protein in HT-22 cells was verified by western blot. Endogenous MAO-A protein levels are the same in all three groups. #: *P*<0.05 versus vehicle-treated control homogenates, (mean±SEM, n=4-5).

Figure 3.9 shows that the PS-1 proteins affects  $\text{Ca}^{2+}$ -sensitive MAO-A activity in HT-22 cells. The cells were transfected with vector, PS-1 wildtype and PS-1(M146V) for 24 hours. Before the activity assay, homogenates were incubated with 1 mM of  $\text{Ca}^{2+}$  (20 min at room temperature). Neither overexpressed PS-1 protein had any effect on basal MAO-A activity [ $F_{(2,20)}=0.399$ ,  $P=0.676$ ], but both PS-1 proteins affected the  $\text{Ca}^{2+}$ -sensitive component of MAO-A activity observed in the vector-transfected control group [ $F_{(1,20)}=6.860$ ,  $P=0.016$ ]. Therefore, exogenous PS-1 (either wildtype or the M146V variant) both affect MAO-A function.

### **3.9 Cell viability of PS-1(M146V)-overexpressing HT-22 cells in the absence and presence of CLG.**

The PS-1 WT and PS-1(M146V) proteins did not alter MTT conversion, used herein as an indicator of mitochondrial integrity and cell viability. Although the selective MAO-A inhibitor CLG tended to increase cell viability and although this tended to be negated by overexpression of the PS-1 proteins, this did not reach statistical significance [ $F_{(5,35)}=1.934$ ,  $P=0.1180$ ] (Figure 3.10).

### **3.10 MAO-A (endogenous and exogenous) co-immunoprecipitates with PS-1 proteins in HT-22 cells.**

The literature suggests that PS-1/ $\gamma$ -secretase can be found in the mitochondria [85, 135] and that the concentration of PS-1 is significantly increased in portions of the endoplasmic reticulum membrane that are closest to mitochondria [136]. Furthermore, protein-protein interactions between the endoplasmic reticulum and the mitochondria are now acknowledged to facilitate inter-organelle communication and metabolic exchange between the two organelles [137]. Given that PS-1 is normally expressed on the endoplasmic reticulum and that MAO-A is expressed on the mitochondria, I chose to examine whether the effects of PS-1 on MAO-A function could be due to a direct interaction between the two proteins. I chose to examine this using either the endogenous proteins or transiently transfected proteins, i.e. a myc-tagged MAO-A protein and a

3XFLAG-tagged PS-1 protein. In the case of the endogenous proteins (MAO-A), I overexpressed untagged PS-1 WT and PS-1(M146V) (in the pcDNA3.1 vector). These

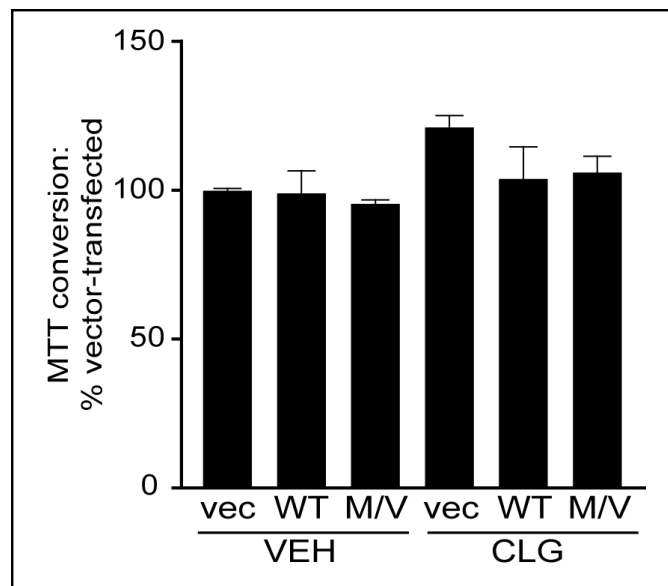
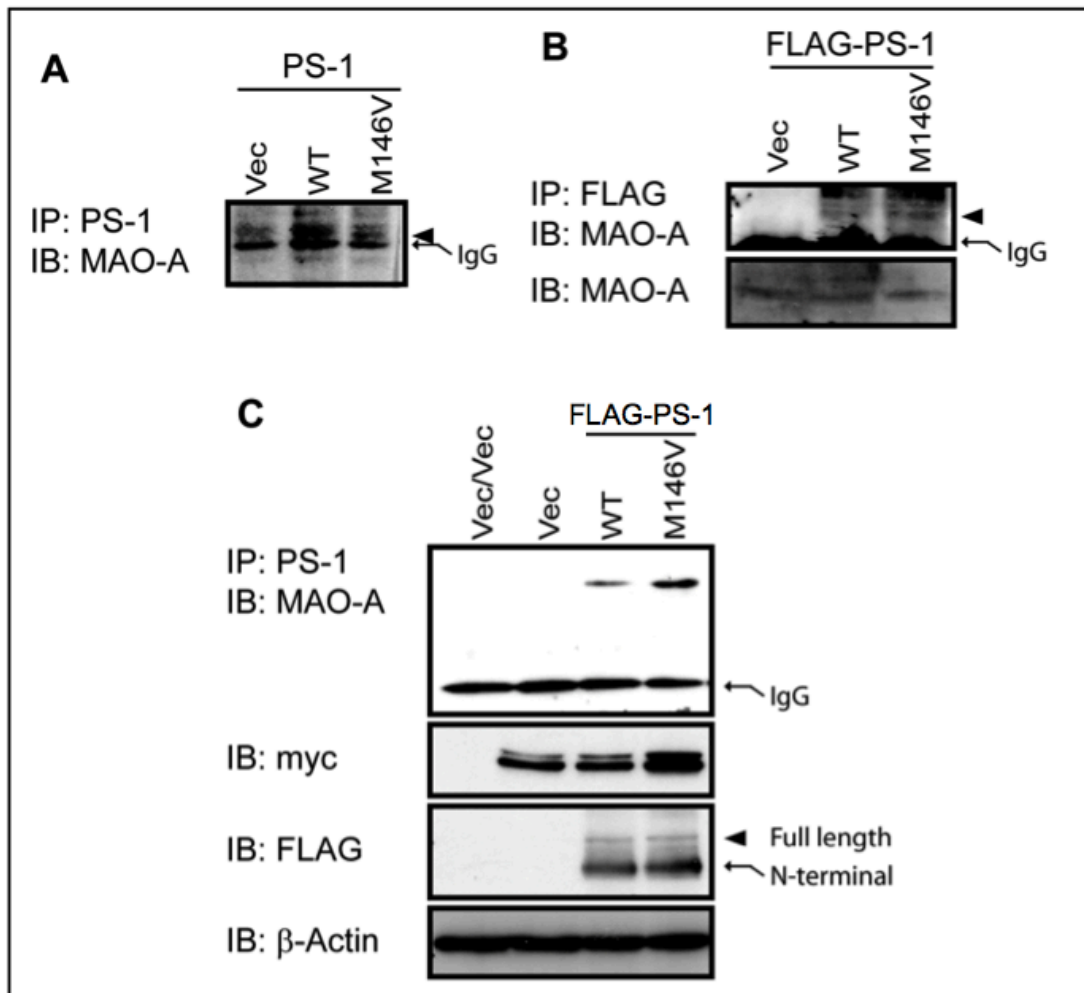


**Figure 3.10: MTT reduction in HT-22 cells overexpressing PS-1 proteins.** There was no effect of either PS-1 wildtype (WT) or PS-1(M146V) (M/V) either alone or in combination with CLG (1  $\mu$ M, 24 h) on MTT reduction in HT-22 cells (mean $\pm$ SEM, n=4-5).



**(previous page)**

**Figure 3.11: MAO-A co-immunoprecipitates with PS-1 proteins in cell cultures.** (A) HT-22 cells were transfected with the empty vector (*vec*) or pcDNA3.1 plasmids coding for PS-1 wildtype (WT) and PS-1(M16V) for 24 h. The protein was extracted and PS-1 was immunoprecipitated. Resolved proteins were probed for *endogenous* MAO-A. (B) HT-22 cells were transfected with the empty FLAG vector (*vec*) or plasmids coding for FLAG-PS-1 wildtype (WT) and FLAG-PS-1(M16V) for 24 h. PS-1 was immunoprecipitated with anti-FLAG. Resolved proteins were probed for *endogenous* MAO-A. (C) HT-22 cells were co-transfected with myc-tagged MAO-A and either the empty FLAG vector (*vec*) or plasmids coding for FLAG-PS-1 wildtype (WT) and FLAG-PS-1(M16V) for 24 h. The *vec/vec* group was transfected with the myc-vector as well as the FLAG-vector and is used as the control group in this experiment. PS-1 was immunoprecipitated with anti-FLAG. Resolved proteins were probed with anti-myc (MAO-A). MAO-A expression was confirmed by probing for myc and PS-1 expression was confirmed by probing for FLAG (revealing the endoproteolytically derived N-terminal fragment).  $\beta$ -Actin was used to demonstrate that equal amounts of protein were loaded in each lane (n=3). IB: Immunoblot/Western blot. IgG: heavy chain of the immunoprecipitating IgG antibody.



proteins were immunoprecipitated using an antibody that was directed towards the loop region of PS-1. The SDS-PAGE resolved proteins were then probed for endogenous MAO-A using the H-70 antibody. MAO-A was detected, albeit very weakly, in both extracts from cultures overexpressing PS-1 proteins (Figure 3.11A). The experiment was repeated, but this time FLAG-tagged PS-1 proteins were overexpressed. MAO-A was again detected in FLAG-immunoprecipitates (Figure 3.11B), but still the detection of MAO-A was relatively weak. A final experiment was performed in which both PS-1 (FLAG-tagged) and MAO-A were overexpressed (Figure 3.11C). In this case, MAO-A expression (detected using the myc antibody) was obvious and was only immunoprecipitated from extracts in which PS-1 WT and PS-1(M146V) were overexpressed. These data strongly support a physical association between PS-1 proteins and MAO-A in HT-22 cells.

### **3.11 DAPT increases MAO-A activity in HT-22 cells and PS-1(M146V) knock-in mice.**

As the possibility that MAO-A protein could be interacting with PS-1 proteins in a non-specific or non-functional manner cannot be fully excluded by co-immunoprecipitation experiments, I chose to use another approach to support my hypothesis that PS-1 and MAO-A interact on a functional level. Since MAO-A function is inhibited by expression of PS-1(M146V) (current thesis; corroborates work done by a previous M.Sc. student in our group [134]), I chose to use a PS-1 inhibitor to determine whether it could influence MAO-A catalytic activity (given the potential for close proximity between the two proteins). I chose to use the semi-peptidic N-[N-(3,5-difluorophenacetyl)-L-alanyl]-S-phenylglycine *t*-butyl ester (DAPT) as it was the first  $\gamma$ -secretase inhibitor to have been studied *in vitro* [138] and is now known to act as a substrate-inhibitor for  $\gamma$ -secretase function [139].

Overexpression of PS-1 proteins tended to increase MAO-A activity [ $F_{(5,17)}=5.945$ ,  $P=0.005$ ], although *post hoc* analysis indicated that this was not significant. In contrast, parallel homogenates incubated with DAPT clearly had significantly enhanced MAO-A activity (Figure 3.12). This supports the observation that

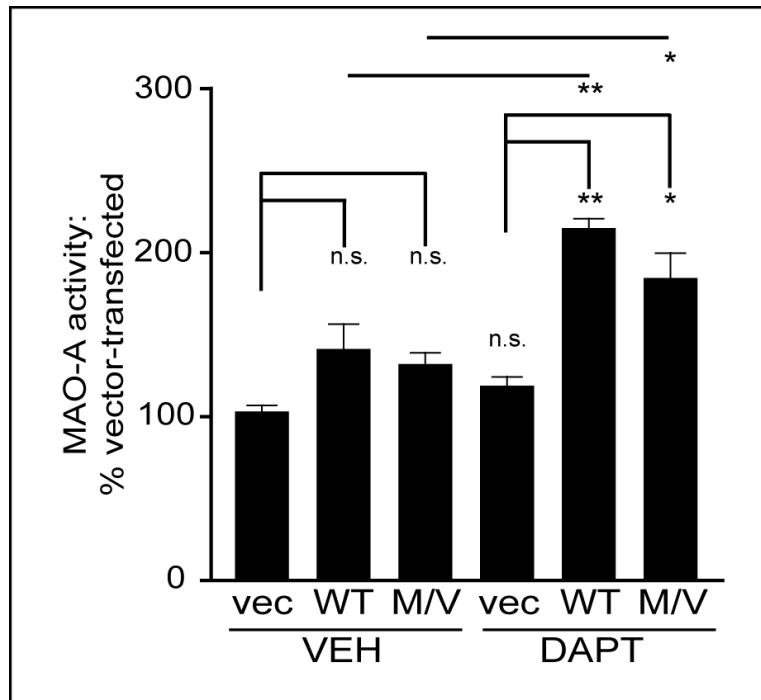


**Figure 3.12: Treatment of PS-1/ $\gamma$ -secretase inhibitor DAPT increases MAO-A activity in HT-22 cells.** HT-22 cell homogenates, from cultures that overexpressed either PS-1 wildtype (WT) or the PS-1(M146V) (M/V) protein, were incubated with the PS-1/ $\gamma$ -secretase inhibitor DAPT at concentration of 1  $\mu$ M. The endogenous MAO-A activity (herein indicated as the activity measured in vehicle (VEH)-treated, vector (vec)-transfected HT-22 cultures) was determined. Compared with the VEH-treated cells, MAO-A activity was not significantly affected by overexpression of either PS-1 WT or PS-1(M146V) proteins alone, but was significantly increased when the corresponding homogenates were treated with DAPT. n.s. = not significant; \*:  $P < 0.05$  & \*\*:  $P < 0.01$  versus vehicle or between indicated groups, (mean $\pm$ SEM, n=4-7).

DAPT also can enhance MAO-A activity in PS-1(M146V) mouse extracts [134]. The use of frozen tissues and incubation of the homogenates with DAPT precludes any events at the transcriptional and translational levels. Therefore, PS-1 must interact with MAO-A *in vivo*.

### **3.12 CLG promotes the interaction between PS-1 and MAO.**

Since incubation of a homogenate with DAPT can increase MAO-A activity, and thus suggests an interaction between PS-1 and MAO-A *in vivo*, I chose to examine whether the PS-1 protein and the MAO-A protein could be co-immunoprecipitated from mouse cortical extracts. Pre-cleared extracts were immunoprecipitated with the PS-1 loop antibody and the SDS-PAGE resolved proteins were probed for MAO-A. Both wildtype PS-1 and PS-1(M146V) were found to co-immunoprecipitate MAO-A (Figure 3.13). At the same time, extracts from CLG-treated mice were also examined. It was noticed that in extracts from these CLG-treated mice the co-immunoprecipitation was enhanced. The middle panel of Figure 3.13 reveals that in pre-cleared tissue lysates, two MAO-A bands were detected and that one of these bands (at ~45 kDa) disappeared with CLG treatment. This suggests the possibility that MAO-A could normally be cleaved and that CLG somehow interferes with this process. The process could be a PS-1-dependent mechanism. The physiological relevance of this remains unclear.

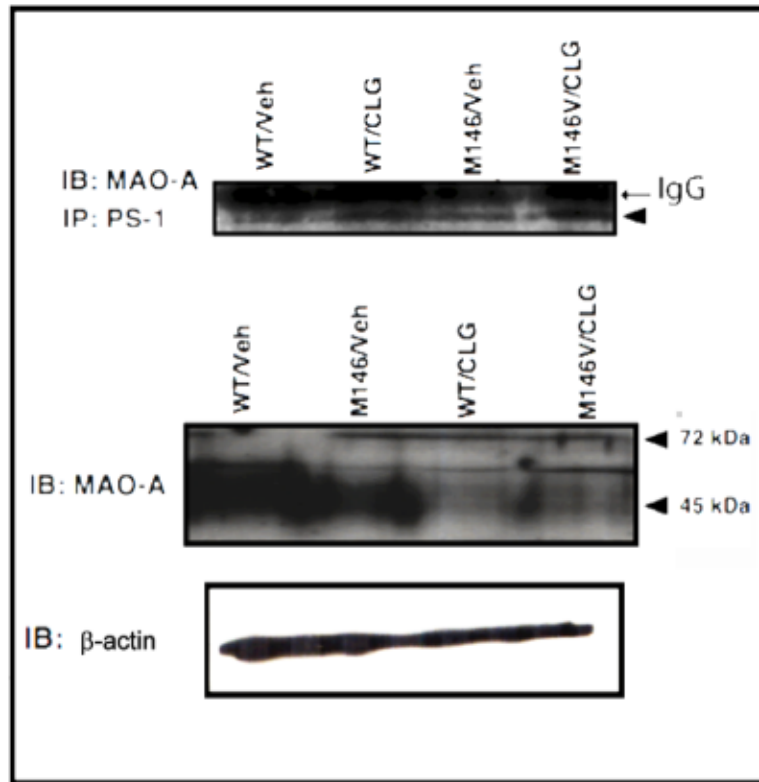


**Figure 3.13: Immunoprecipitation assay for PS-1 and MAO-A in CLG treated/non-CLG-treated PS-1 wildtype or PS-1(M146V) mouse cortex.** PS-1 was immunoprecipitated (anti-loop) from cortical extracts and resolved proteins were probed for MAO-A. These preliminary results reveal that in CLG-treated animals, PS-1 interacted more with MAO-A protein (top panel). At the same time, a 46 kDa band was lost in these two sample detected by immune blot (IB) (middle panel).

### **Part III: Mapping the potential motif for interaction between PS-1 and MAO-A**

The above preliminary data suggest that PS-1 could be mediating a MAO-A cleavage event. Alignment of the primary amino acid sequence of MAO-A and MAO-B confirms the high sequence identity between these two proteins, and when aligned with APP (substrate for PS-1/ $\gamma$ -secretase cleavage), it becomes apparent that there is some sequence identity in the region highlighted in Figure 3.14. Furthermore, both MAO-A and MAO-B contain a motif that is very similar to the “GVVIA” motif that is targeted by PS-1/ $\gamma$ -secretase to release the A $\beta$ (1-40) and A $\beta$ (1-42) peptides that are thought to be central to AD-related pathology. Cleavage of APP after “GVV” releases the A $\beta$ (1-40) fragment; cleavage after the “VIA” releases the A $\beta$ (1-42) fragment. Since there is only one amino acid different within this motif between MAO-A and MAO-B, we have mutated the “A” (alanine) to “S” (serine) in the MAO-A protein; this strategy gives an MAO-A protein that contains the MAO-B “GSVIK” motif. The same strategy was used to mutate the MAO-B protein such that it now contains the MAO-A “GAVIK” motif. Note that the Alanine residue in MAO-A is residue 302, whereas the corresponding residue in MAO-B, i.e. the serine, is residue 293. I chose to determine whether these substitutions would affect the function of either MAO-A or MAO-B.

#### **3.13 Chromatogram sequences of MAO-A A302S and MAO-B S293A.**

The mutation in MAO-A (to give the A302S substitution) was confirmed by DNA sequencing (Figure 3.15). The mutation in MAO-B (to give the S293A substitution) was also confirmed by DNA sequencing (Figure 3.15). The gene mutation was achieved using Stratagene’s QuikChange® Site-Directed Mutagenesis Kit.

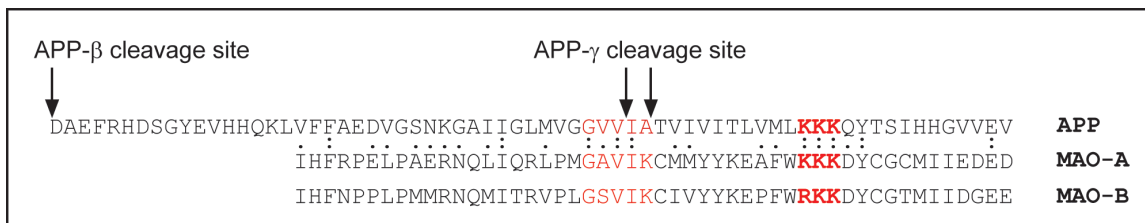


**Figure 3.14: MAO-A contains a putative PS-1 binding site.** Alignment of the MAO-A and MAO-B primary amino acid sequences not only confirm their high sequence identity, but also reveals that both MAO-A and MAO-B contain a motif “GA/SVIK” that is very similar to the “GVVIA” motif in APP that is targeted for cleavage by PS-1/γ-secretase. Cleavage of APP after “GVV” releases the Aβ(1-40) fragment; cleavage after the “VIA” releases the Aβ(1-42) fragment. The highlighted “KKK” is the recognized highly charged portion (anchor) of the transmembrane domain of the APP protein.

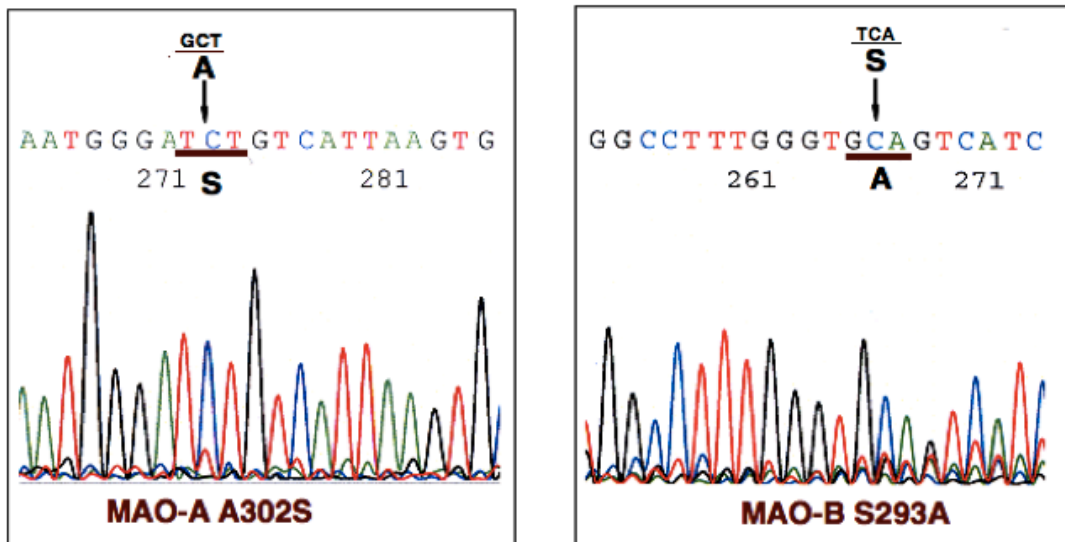


**Figure 3.15: Sequencing of targeted codon substitutions in *MAO-A* and *MAO-B*.** (left) Chromatograms show the mutated codon in MAO-A (TCT=Serine, S) and (right) the corresponding mutated codon in MAO-B (GCA=Alanine, A). The wildtype codons GCT (=Alanine, A) in MAO-A and TCA (=Serine, S) in MAO-B are indicated immediately above the mutated ones.

### **3.14 Molecular evidence of the PS-1 targeting motif in MAO-A.**

MAO-A(A302S) and MAO-B(S293A) and the corresponding wildtype proteins were overexpressed in N2a cells for 24 hours (Figure 3.16A,B). N2a cells were used for this study as they are functionally MAO-A null [128] and are therefore a good model to test the activity of overexpressed MAO-A proteins. Immuno/Western blot confirmed the expression and revealed that the single amino acid substitution did not affect expression levels of the respective proteins. Assaying for catalytic activity reveals that the A-to-S substitution increases MAO-A activity by approximately 25% (Figure 3.16C), but also interferes with the interaction between PS-1 and MAO-A (Figure 3.16E). MAO-B activity (estimated using [<sup>14</sup>C-phenylethylamine] as substrate) reveals that the S-to-A substitution in MAO-B results in a decrease of approximately 50% (Figure 3.16D).

### **3.15 MAO-A activity in HT-22 cultures is increased by expression of depression-related PS-1 mutants.**

Wildtype PS-1 and the PS-1(A431E) and PS-1(L235V) variants that have been associated with an increase in the incidence of depression in pre-demented patients [2] were overexpressed in HT-22 cells for 24 hours (Figure 3.17). These proteins exerted an effect on endogenous MAO-A activity [ $F_{(3,22)}=3.985$ ,  $P=0.0233$ ]. MAO-A activity was increased by the PS-1(A431E) protein (Figure 3.17), thus suggesting that this mutant may play a direct role in the aminergic dysregulation associated with depression in the carriers of this mutation. In contrast, while overexpression of the PS-1(L285V) protein did exert a minor effect on MAO-A activity, this was clearly not significant. This suggests that different PS-1 mutants could exert distinct effects on MAO-A *in vivo* and hence employ distinct mechanisms to induce depression in the carriers of the respective mutations.



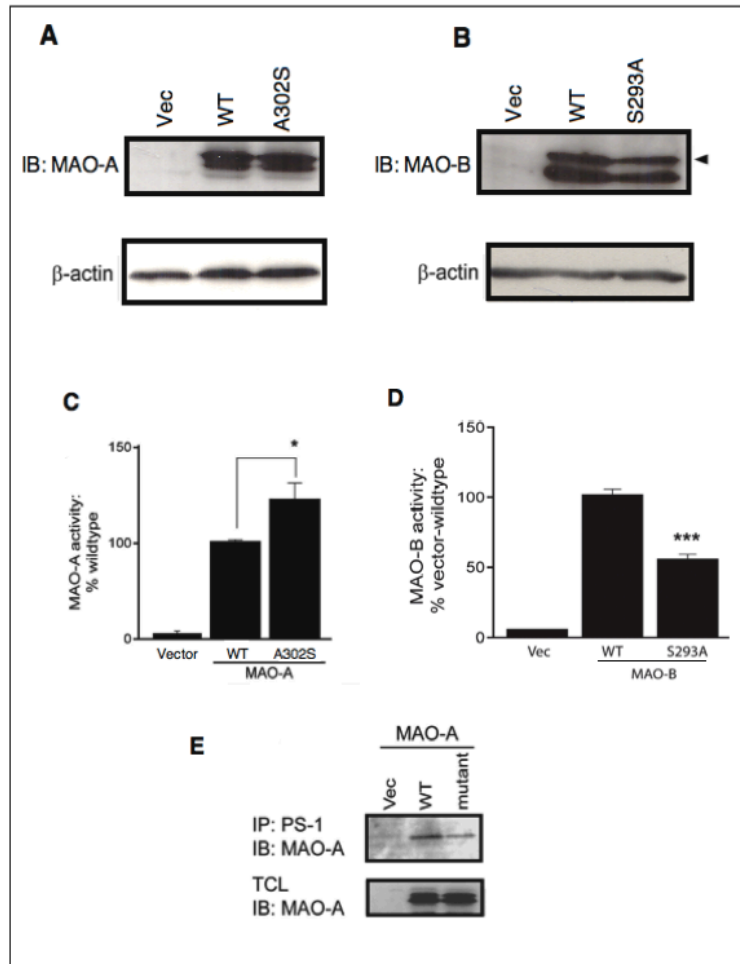


**Figure 3.16: Molecular evidence of a putative PS-1 targeting motif in MAO-A.** (A) MAO-A(A302S) and (B) MAO-B(S293A) and the corresponding wildtype (WT) proteins were overexpressed in N2a cells for 24 hours. Immunoblot (IB) demonstrated that the substitution does not affect protein expression. (C) MAO-A activity was enhanced by substitution of “A” to “S” while (D) MAO-B activity was decreased substitution of “S” to “A”. (E) The co-immunoprecipitation between PS-1 and MAO-A in N2a cells is diminished in cells overexpressing MAO-A(A302S) compared to MAO-A wildtype. \*:  $P < 0.05$  and \*\*\*:  $P < 0.001$ , versus the corresponding WT-transfected (mean $\pm$ SEM, n=3).

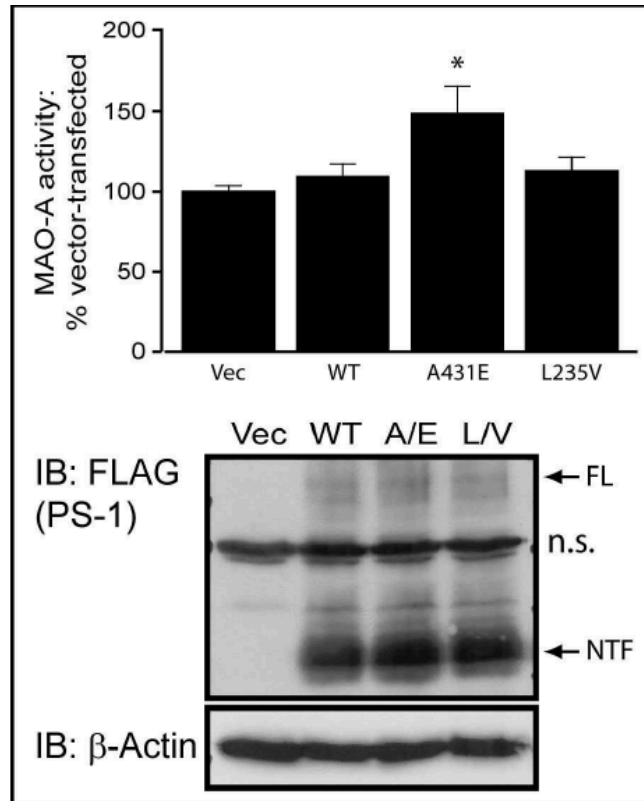


**Figure 3.17: MAO-A activity is increased by overexpression of a depression-related PS-1 mutant.** The vector, PS-1 wildtype, and two PS-1 variants [PS-1(A431E), A/E; PS-1(L235V), L/V) were transfected into HT-22 cell line for 24 hours. The immunoblot (IB) confirms the overexpression of the FLAG-tagged PS-1 proteins (FL: full length; NTF: N-terminal fragment). Levels of  $\beta$ -Actin demonstrate equal protein loading in all four lanes. The endogenous MAO-A activity was then measured. MAO-A activity of cells overexpressing PS-1(A431E) was increased approximately 50%, while the activity in cells overexpressing PS-1(L235V) did not change compared with cells overexpressing the PS-1 wildtype (WT) protein. n.s.: non-specific band. . \*:  $P < 0.05$  versus vector (VEC)-transfected (mean $\pm$ SEM, n=9-10).

#### 4. Discussion.

As early as 1996, early mood changes, including depression, had been found to be a common symptom in AD patients [2]. Neurochemical changes, particularly with monoamines such as serotonin and noradrenaline, have long been associated with some of the earliest events in AD [60]. AD is a multi-factorial disease, which includes influences by genetics, cerebrovascular disease and age, and unfortunately the clinical symptoms of the disease usually present 20-30 years after the onset of pathological changes. Therefore, AD is still a not curable neurodegenerative disease due to the lack of a targetable system. However, discovery of the link between a history of depression and AD possibly suggests a common mechanism, especially one that occurs at an early stage of the development of the disease. The main substrate of MAO-A, *i.e.* serotonin/5-HT, is implicated in major depression [17]. MAO-A is also thought to contribute to oxidative stress through the production of hydrogen peroxide as a natural by-product of the degradation of monoamines. With this in mind, perhaps it is not surprising that some of the most vulnerable cells in the AD brain are cells that are highly immunoreactive for MAO-A [29]. This thesis work was an extension of the work previously undertaken by a Master's student in our laboratory [134]. Since people with a history of depression tend to be at higher risk for developing AD and that certain PS-1 mutants are reportedly associated with an increase in depression [2], I hypothesized that PS-1 mutants could contribute to changes in biogenic amine function at early stages of the disease. These changes could not only lead to depression, but ultimately could lead to neurotoxicity (increased MAO-A-mediated oxidative stress) and AD.

PS-1 is the catalytic core of the  $\gamma$ -secretase complex, which plays an important role in the APP cleavage process and produces  $\beta$ -amyloid protein ( $A\beta$ ). Since  $A\beta$  accumulation is thought to be a key step in the pathogenesis of AD, most of the literature focuses more on the APP/PS-1 double transgenic mouse models that have an exaggerated  $A\beta$  burden because of the expression of the two mutant proteins. However,  $A\beta$  is usually produced in the late stage of AD, well after neurochemical changes and neurodegeneration. In these animal models, monoamine levels change [140, 141]. While these monoamines, *e.g.* serotonin and norepinephrine (NE), are known substrates of

MAO-A, it is surprising that the function of MAO-A in these animals has never been examined (or perhaps simply not reported). I used the commercially available PS-1(M146V) knock-in mice to do the current thesis work as it provides a nice platform to investigate how an AD-related PS-1 protein could (on its own) affect MAO-A function.

In order to determine if wildtype PS-1 animals are different from the PS-1(M146V) knock-in littermates, cortical and cerebellar tissues were assayed for MAO-A activity. As the literature suggests that the PS-1(M146V) mutation can induce a significant disruption of  $\text{Ca}^{2+}$  homeostasis [142-144], both basal and  $\text{Ca}^{2+}$ -sensitive MAO-A activity [128, 129] was examined. In the PS-1(M146V) mice, basal cortical MAO-A activity was increased by approximately 10% while the  $\text{Ca}^{2+}$ -sensitive component to MAO-A activity was increased approximately 30%. Moreover, this increasing  $\text{Ca}^{2+}$ -sensitivity of MAO-A occurred in an age- and region-dependent manner (i.e. no changes were observed in cerebellum). Interestingly, when we looked at the level of expression of the MAO-A protein, there was approximately 50% more MAO-A protein when compared to MAO-A expression in wildtype mice. The mismatch between MAO-A protein and activity suggested the possibility of some posttranslational event(s) regulating MAO-A function. Whether this is occurring while MAO-A is expressed within the mitochondria or whether this is occurring when MAO-A is being processed through the endoplasmic reticulum and golgi apparatus is unclear. The presence of an active overexpressed MAO-A protein in these cells suggested that MAO-A is expressed on the mitochondria. This, then, suggested that the effect of PS-1 is between organelles.

The disturbed laminar architecture in the PS-1(M146V) mouse cortex, in comparison to the wildtype animal, is another example of subtle effects of this transgene on the central nervous system. The PS-1 protein is not simply involved in the neuropathology that accompanies AD [145], but is also required for the normal development of the cerebral cortex [146, 147]. The patchy distribution of Nissl substance and disrupted laminar boundaries in the cortices of PS-1(M146V) mice was consistent with reports using prenatal PS-1-null mice [148] and postnatal PS-1 conditional knockout mice [147]; *a priori*, if PS-1(M146V) is inhibiting MAO-A, as the current activity data indicate, then a role for a PS-1(M146V)-mediated inhibition of MAO-A in laminar disorganization is possible. This is supported indirectly by the cytoarchitectural changes

observed in the cortex of MAO-A-knockout mice [44] and following MAO-A inhibition and hyperserotonergic (but not noradrenergic) function during the first week of life in wildtype mice [149].

To study if MAO-A-dependent behaviour correlated with the expression of the PS-1(M146V) protein, the mice were subjected to the forced swim test (a test of non-cognitive behaviours in rodents). The PS-1 transgene did not cause any behavioural phenotype on its own. However when the mice were treated with the selective MAO-A inhibitor CLG, a significant decrease of the time that the PS-1(M146V) mice spent swimming was observed. The fact that CLG treatment increased the duration of immobility in the forced swim test, rather than decreasing it (which would be the typical profile of an “antidepressant” drug) was somewhat unexpected, but this did support reports that MAO inhibitors do not consistently give a “positive” result in this test [reviewed in [150]]. Combining this with the region- and age-dependent activity change, as well as change of protein distribution, it would be reasonable to assume that PS-1(M146V) transgene does affect MAO-A function in these animals to a certain extent and would therefore affect the level of neurochemistry of the brain, especially aminergic substrates. Indeed, HPLC analysis of monoamines and selected metabolites demonstrated a significant decrease in cortical levels of 5-HIAA (an MAO-A-mediated metabolite of 5-HT). The decreased levels of 5-HIAA were not due to a lower 5-HT synthesis or its precursor tryptophan because a parallel increase in levels of 5-HT was observed. This supported the notion that MAO-A function was inhibited in a PS-1(M146V) background.

Cognitive dysfunction is characteristic of the later stages of clinical AD. Yet earlier stages of AD are associated more often with several non-cognitive symptoms including depression [151]. Given that depression does respond to MAO-A inhibition and that depression is associated with region-specific noradrenergic and serotonergic etiologies, it is not surprising that acute CLG treatment would affect both noradrenergic and serotonergic metabolism in the PS-1(M146V) mice. The fact that noradrenergic changes were not only region-dependent, but also were greater than serotonergic changes, is also not unexpected [152, 153]. Indeed, *acute* CLG treatment is known to elicit some off-target effects on the noradrenergic synthetic enzyme, tyrosine hydroxylase [154]. Exacerbated changes in noradrenergic and serotonergic metabolism following

acute CLG treatment in PS-1(M146V) mice could certainly contribute to the changes in non-cognitive symptoms (defined herein by the forced-swim test).

Mutation-induced changes in the conformation of the PS-1 protein are known to exist [155]. Perhaps by virtue of a direct association between PS-1(M146V) and MAO-A, a change in the structure of MAO-A could ensue and this could explain the increased potency of CLG in the PS-1(M146V) mouse cortical and cerebellar samples. A conformational change in the MAO-A protein could certainly alter the accessibility of CLG to its binding site, which could promote an apparent change in the Hill slope without significantly shifting the  $IC_{50}$  for CLG towards MAO-A. While this suggests partially interconvertible states of a single CLG binding site, it could also be indicating a PS-1-dependent post-translational mechanism. In support of the latter possibility, PS-1 variants are known to activate distinct signalling cascades [156], several of which have been found by our research group to affect MAO-A function [128].

The potential for post-translational modification also suggests the possibility for a direct influence of the PS-1 protein on MAO-A function. At this point, I chose to continue characterizing the influence of PS-1 on MAO-A using overexpression strategies in cell cultures.

The data collected from the mice suggested significant differences between PS-1 wildtype and PS-1(M146V) proteins in terms of their effect(s) on MAO-A function. In the immortalized neuronal HT-22 cell line, the overexpression of both PS-1 wildtype and PS-1(M146V) proteins diminished the  $Ca^{2+}$ -sensitive component to MAO-A activity. The reason for the different tendencies in cell cultures *versus* animal tissue could be due to the transient expression (in cell cultures) compared with six months of expression in the PS-1(M146V) mice. Furthermore, the cell culture is clonal (i.e. one cell type), whereas the results from the tissues represent the average response of all cell types in that tissue. The toxicity of PS-1 mutants was also determined using MTT conversion as an indirect indicator of cell viability. A decrease in viability of cells overexpressing either PS-1 wildtype or the PS-1(M146V) proteins was observed, but only the PS-1(M146V)-induced effect was sensitive to inhibition of MAO-A. Although the reason for the differences remains unclear, what can be concluded from the cell-based assays is that PS-1 proteins can exert MAO-A-sensitive effects *in vitro*. The observation that the MAO-A protein

could be co-immunoprecipitated by PS-1 was strong evidence that the effect of PS-1 proteins could be due to a direct association between the two proteins. Although this was initially unexpected, the literature does support the possibility that proteins expressed on the endoplasmic reticulum can interact directly with mitochondrial proteins [137]. The possibility that PS-1 could be similarly influencing mitochondrial proteins is supported by several lines of evidence including (a) the concentration of PS-1 proteins in the endoplasmic reticulum membranes that are closest to the mitochondria [136] and (b) the detection of PS-1 and other components of the  $\gamma$ -secretase complex in the mitochondrial fraction [85, 135]. A direct association between PS-1 proteins and MAO-A was further supported by the ability of the  $\gamma$ -secretase substrate-competitor DAPT [139] to increase MAO-A activity in both cell cultures (current thesis) and PS-1(M146V) mouse cortical homogenates [134]. This appeared to suggest that DAPT, by binding with the C-terminal of PS-1, is blocking the access of substrate to MAO-A. When MAO-A is no longer associated with PS-1/ $\gamma$ -secretase because of competition by DAPT, then MAO-A activity is enhanced. This indirectly confirmed that PS-1(M146V) inhibits MAO-A activity *in vivo* (which is the conclusion drawn from the mismatch between MAO-A protein and MAO-A activity in the PS-1(M146V) cortical homogenates).

A previous Master's thesis from this laboratory [134] demonstrated that overexpression of the AD-associated PS-1 mutants, such as the highly aggressive PS-1(Y115H) protein, can lead to the cleavage of MAO-A to form a C-terminal fragment [134]. If it is true, then MAO-A could be a novel substrate for PS-1/ $\gamma$ -secretase. Based on alignments of MAO-A and MAO-B (and the well-known substrate APP), a putative PS-1 binding/cleavage site was identified. As MAO-B does not appear to associate as readily with PS-1 [134] and this putative cleavage site in MAO-A and MAO-B differs by a single amino acid, substitution mutants were generated such that MAO-A contained the MAO-B-specific amino acid (and MAO-B contained the MAO-A-specific amino acid). In keeping with PS-1 possibly inhibiting MAO-A function, the A-to-S substitution in MAO-A not only increased the catalytic activity of the overexpressed MAO-A protein, but this protein also interacted less with PS-1 (determined by co-immunoprecipitation experiments). In contrast, the complementary substitution in MAO-B decreased the catalytic activity of the overexpressed MAO-B protein. Work in the laboratory is

currently underway to determine whether this substitution affects the ability of MAO-B to interact with PS-1 protein(s).

Mutated forms of PS-1 have been associated with particularly aggressive forms of AD. The fact that some of these mutations have also been associated with depression in pre-demented AD patients is very exciting. This suggests that depression and AD might share a common causative biochemical mechanism. The evidence provided herein supports a role for PS-1 proteins in MAO-A function both *in vivo* and *in vitro*. It is worth noting that different forms of PS-1 mutant may cause very different effects on MAO-A function. Obviously, the PS-1(M146V) protein inhibited MAO-A. The PS-1(A431E) protein (but *a priori* not the PS-1(L285V) protein), both of which have been reported to induce a clinical depression phenotype [2], activated MAO-A. This needs to be examined more closely, but differences in the effects of PS-1 variants on cellular mechanisms and phenotypes are well documented and a direct role for some of these variants in depression is certainly feasible, although multiple mechanisms of actions might be involved (direct and/or indirect), including mechanisms dependent on MAO-A dysfunction. Further examination of this interesting and unique endogenous means of regulating MAO-A function, as well as its relation to clinically relevant pathologies, including depression and AD, is clearly warranted.

## 5. Future Directions

The current study has demonstrated an endogenous mechanism of regulating MAO-A function by PS-1 proteins. As a binding partner of  $\gamma$ -secretase, a potential binding motif of MAO-A was also studied in this thesis. However some further experiments are still needed to prove the interaction between the two proteins. First, the co-localization of PS-1 and MAO-A in AD/depression-related brain has not been fully established. Therefore, it would be important to monitor the subcellular localization of the two proteins, not only to determine where they are expressed, but also if they affect each other's processing and/or transport. Second, a potential MAO-A C-terminal cleavage product was observed both *in vivo* and *in vitro* by immunoblot. As such, further studies are needed to confirm that these detected bands indeed represent smaller MAO-A species or fragments. The putative binding site in MAO-A identified in this thesis project



could be helpful to examine this potential cleavage process. Third, the potential change of conformation in MAO-A, as suggested by the increased potency of CLG in the PS-1(M146V) mice, needs to be examined as it would be important to understand how MAO-A structure could be affected by binding with PS-1. This would also be very useful in characterizing the binding parameters needed for the association between PS-1 and MAO-A. Fourth, we noticed that in PS-1(M146V) knock-in mice, there was a significant increase in MAO-A protein, but that there was no corresponding change in MAO-A activity. Further understanding of the mechanism underlying the mismatch between protein and function would be important, as would its contribution to MAO-A protein turnover in the AD-related mouse and, ultimately, in the human condition. Finally, our data also suggested that different PS-1 mutants might be eliciting different effects on MAO-A function. Therefore, more animal models expressing PS-1 mutant proteins, especially the highly aggressive (and commercially available) PS-1( $\Delta$ Ex9) variant, should also be examined.

## References

1. JK Walsh, RM Benca, M Bonnet, DJ Buysse, PJ Hauri, J Kiley, A Monjan, CM Morin, JG Ricca, S Rogus, et al: **Insomnia: assessment and management in primary care.** *Sleep* 1999, **22 Suppl 2**:S402-8.
2. JM Ringman, C Diaz-Olavarrieta, Y Rodriguez, M Chavez, F Paz, J Murrell, MA Macias, M Hill, C Kawas: **Female preclinical presenilin-1 mutation carriers unaware of their genetic status have higher levels of depression than their non-mutation carrying kin.** *Journal of Neurology Neurosurgery and Psychiatry* 2004, **75**:500-502.
3. GE Berrios: **Melancholia and depression during the 19th century: a conceptual history.** *Br J Psychiatry* 1988, **153**:298-304.
4. J Radden: **Moody minds distempered : essays on melancholy and depression.** Oxford ; New York: Oxford University Press; 2009.
5. JJ Schildkraut: **The catecholamine hypothesis of affective disorders: a review of supporting evidence.** *Am J Psychiatry* 1965, **122**:509-22.
6. M Fava, KS Kendler: **Major depressive disorder.** *Neuron* 2000, **28**:335-41.
7. MM Weissman, M Olfson: **Depression in women: implications for health care research.** *Science* 1995, **269**:799-801.
8. AF Tarbuck, ES Paykel: **Effects of major depression on the cognitive function of younger and older subjects.** *Psychol Med* 1995, **25**:285-95.
9. E Falkum, G Pedersen, S Karterud: **Diagnostic and Statistical Manual of Mental Disorders, Fourth Edition, paranoid personality disorder diagnosis: a unitary or a two-dimensional construct?** *Comprehensive Psychiatry* 2009, **50**:533-541.
10. RE Wragg, DV Jeste: **Overview of depression and psychosis in Alzheimer's disease.** *Am J Psychiatry* 1989, **146**:577-87.
11. RC Kessler: **Epidemiology of women and depression.** *J Affect Disord* 2003, **74**:5-13.

12. JR Lacasse, J Leo: **Serotonin and depression: a disconnect between the advertisements and the scientific literature.** *PLoS Med* 2005, **2**:e392.
13. J Mendels, JL Stinnett, D Burns, A Frazer: **Amine precursors and depression.** *Arch Gen Psychiatry* 1975, **32**:22-30.
14. N Risch, R Herrell, T Lehner, KY Liang, L Eaves, J Hoh, A Griem, M Kovacs, J Ott, KR Merikangas: **Interaction Between the Serotonin Transporter Gene (5-HTTLPR), Stressful Life Events, and Risk of Depression: A Meta-analysis (vol 301, pg 2462, 2009).** *Jama-Journal of the American Medical Association* 2009, **302**:492-492.
15. SO Moldin, WA Scheftner, JP Rice, E Nelson, MA Knesevich, H Akiskal: **Association between Major Depressive Disorder and Physical Illness.** *Psychological Medicine* 1993, **23**:755-761.
16. ICG Weaver: **Epigenetic programming by maternal behavior and pharmacological intervention - Nature versus nurture: Let's call the whole thing off.** *Epigenetics* 2007, **2**:22-28.
17. A Coppen: **The biochemistry of affective disorders.** *Br J Psychiatry* 1967, **113**:1237-64.
18. JJ Schildkraut: **The catecholamine hypothesis of affective disorders: a review of supporting evidence. 1965.** *J Neuropsychiatry Clin Neurosci* 1995, **7**:524-33; discussion 523-4.
19. P Blier, NM Ward: **Is there a role for 5-HT1A agonists in the treatment of depression?** *Biol Psychiatry* 2003, **53**:193-203.
20. JG Hensler: **Differential regulation of 5-HT1A receptor-G protein interactions in brain following chronic antidepressant administration.** *Neuropsychopharmacology* 2002, **26**:565-73.
21. JH Meyer, N Ginovart, A Boovariwala, S Sagrati, D Hussey, A Garcia, T Young, N Praschak-Rieder, AA Wilson, S Houle: **Elevated monoamine oxidase A levels in the brain - An explanation for the monoamine imbalance of major depression.** *Archives of General Psychiatry* 2006, **63**:1209-1216.
22. AS Elhwuegi: **Central monoamines and their role in major depression.** *Prog Neuropsychopharmacol Biol Psychiatry* 2004, **28**:435-51.

23. M Bortolato, K Chen, JC Shih: **Monoamine oxidase inactivation: from pathophysiology to therapeutics.** *Adv Drug Deliv Rev* 2008, **60**:1527-33.
24. J Knoll, K Magyar: **Some puzzling pharmacological effects of monoamine oxidase inhibitors.** *Adv Biochem Psychopharmacol* 1972, **5**:393-408.
25. HL White, AT Glassman: **Multiple binding sites of human brain and liver monoamine oxidase: substrate specificities, selective inhibitions, and attempts to separate enzyme forms.** *J Neurochem* 1977, **29**:987-97.
26. JW Greenawalt, C Schnaitman: **An appraisal of the use of monoamine oxidase as an enzyme marker for the outer membrane of rat liver mitochondria.** *J Cell Biol* 1970, **46**:173-9.
27. JL Sullivan, JO Cavenar, Jr., CN Stanfield, EB Hammett: **Reduced MAO activity in platelets and lymphocytes of chronic schizophrenics.** *Am J Psychiatry* 1978, **135**:597-8.
28. JW Jahng, TA Houpt, TH Joh, JH Son: **Differential expression of monoamine oxidase A, serotonin transporter, tyrosine hydroxylase and norepinephrine transporter mRNA by anorexia mutation and food deprivation.** *Brain Res Dev Brain Res* 1998, **107**:241-6.
29. J Saura, JM Luque, AM Cesura, M Da Prada, V Chan-Palay, G Huber, J Loffler, JG Richards: **Increased monoamine oxidase B activity in plaque-associated astrocytes of Alzheimer brains revealed by quantitative enzyme radioautography.** *Neuroscience* 1994, **62**:15-30.
30. KN Westlund, RM Denney, RM Rose, CW Abell: **Localization of distinct monoamine oxidase A and monoamine oxidase B cell populations in human brainstem.** *Neuroscience* 1988, **25**:439-56.
31. AM O'Carroll, CJ Fowler, JP Phillips, I Tobbia, KF Tipton: **The deamination of dopamine by human brain monoamine oxidase. Specificity for the two enzyme forms in seven brain regions.** *Naunyn Schmiedebergs Arch Pharmacol* 1983, **322**:198-202.
32. V Glover, M Sandler, F Owen, GJ Riley: **Dopamine is a monoamine oxidase B substrate in man.** *Nature* 1977, **265**:80-1.

33. CJ Fowler, TJ Mantle, KF Tipton: **The nature of the inhibition of rat liver monoamine oxidase types A and B by the acetylenic inhibitors clorgyline, l-deprenyl and pargyline.** *Biochem Pharmacol* 1982, **31**:3555-61.
34. KF Tipton, AM O'Carroll, JM McCrodden: **The catalytic behaviour of monoamine oxidase.** *J Neural Transm Suppl* 1987, **23**:25-35.
35. JP Johnston: **Some observations upon a new inhibitor of monoamine oxidase in brain tissue.** *Biochem Pharmacol* 1968, **17**:1285-97.
36. W Birkmayer, P Riederer, MB Youdim, W Linauer: **The potentiation of the anti akinetik effect after L-dopa treatment by an inhibitor of MAO-B, Deprenil.** *J Neural Transm* 1975, **36**:303-26.
37. AW Bach, NC Lan, DL Johnson, CW Abell, ME Bembenek, SW Kwan, PH Seeburg, JC Shih: **cDNA cloning of human liver monoamine oxidase A and B: molecular basis of differences in enzymatic properties.** *Proc Natl Acad Sci U S A* 1988, **85**:4934-8.
38. JC Shih, K Chen, RM Geha: **Determination of regions important for monoamine oxidase (MAO) A and B substrate and inhibitor selectivities.** *J Neural Transm Suppl* 1998, **52**:1-8.
39. Y Tsugeno, I Hirashiki, F Ogata, A Ito: **Regions of the molecule responsible for substrate specificity of monoamine oxidase A and B: a chimeric enzyme analysis.** *J Biochem* 1995, **118**:974-80.
40. C Binda, P Newton-Vinson, F Hubalek, DE Edmondson, A Mattevi: **Structure of human monoamine oxidase B, a drug target for the treatment of neurological disorders.** *Nat Struct Biol* 2002, **9**:22-6.
41. J Ma, F Kubota, M Yoshimura, E Yamashita, A Nakagawa, A Ito, T Tsukihara: **Crystallization and preliminary crystallographic analysis of rat monoamine oxidase A complexed with clorgyline.** *Acta Crystallogr D Biol Crystallogr* 2004, **60**:317-9.
42. L De Colibus, M Li, C Binda, A Lustig, DE Edmondson, A Mattevi: **Three-dimensional structure of human monoamine oxidase A (MAO A):**

- relation to the structures of rat MAO A and human MAO B.** *Proc Natl Acad Sci U S A* 2005, **102**:12684-9.
43. MB Youdim, YS Bakhle: **Monoamine oxidase: isoforms and inhibitors in Parkinson's disease and depressive illness.** *Br J Pharmacol* 2006, **147 Suppl 1**:S287-96.
44. O Cases, I Seif, J Grimsby, P Gaspar, K Chen, S Pournin, U Muller, M Aguet, C Babinet, JC Shih, et al: **Aggressive-Behavior and Altered Amounts of Brain-Serotonin and Norepinephrine in Mice Lacking Maa.** *Science* 1995, **268**:1763-1766.
45. JC Shih, MJ Ridd, K Chen, WP Meehan, MP Kung, I Seif, E De Maeyer: **Ketanserin and tetrabenazine abolish aggression in mice lacking monoamine oxidase A.** *Brain Res* 1999, **835**:104-12.
46. HG Brunner, M Nelen, XO Breakefield, HH Ropers, BA van Oost: **Abnormal behavior associated with a point mutation in the structural gene for monoamine oxidase A.** *Science* 1993, **262**:578-80.
47. HG Brunner, MR Nelen, P van Zandvoort, NG Abeling, AH van Gennip, EC Wolters, MA Kuiper, HH Ropers, BA van Oost: **X-linked borderline mental retardation with prominent behavioral disturbance: phenotype, genetic localization, and evidence for disturbed monoamine metabolism.** *Am J Hum Genet* 1993, **52**:1032-9.
48. NI Dubrovina, NK Popova, MA Gilinskii, RA Tomilenko, I Seif: **Acquisition and extinction of a conditioned passive avoidance reflex in mice with genetic knockout of monoamine oxidase A.** *Neurosci Behav Physiol* 2006, **36**:335-9.
49. JJ Kim, JC Shih, K Chen, L Chen, S Bao, S Maren, SG Anagnostaras, MS Fanselow, E De Maeyer, I Seif, et al: **Selective enhancement of emotional, but not motor, learning in monoamine oxidase A-deficient mice.** *Proc Natl Acad Sci U S A* 1997, **94**:5929-33.
50. ABB Jones, CMB Pare, RS Stacey, K Price, Nicholso.Wj: **Brain Amine Concentrations after Monoamine-Oxidase Inhibitor Administration.** *British Medical Journal* 1972, **1**:17-&.

51. MC Anderson, F Hasan, JM McCrodden, KF Tipton: **Monoamine oxidase inhibitors and the cheese effect.** *Neurochem Res* 1993, **18**:1145-9.
52. A Colzi, F Dagostini, AM Cesura, E Borroni, M Daprada: **Monoamine Oxidase-a Inhibitors and Dopamine Metabolism in Rat Caudatus - Evidence That an Increased Cytosolic Level of Dopamine Displaces Reversible Monoamine Oxidase-a Inhibitors In vivo.** *Journal of Pharmacology and Experimental Therapeutics* 1993, **265**:103-111.
53. JR Davidson: **Pharmacotherapy of social phobia.** *Acta Psychiatr Scand Suppl* 2003:65-71.
54. R Amrein, W Hetzel, M Stabl, W Schmid-Burgk: **RIMA--a new concept in the treatment of depression with moclobemide.** *Int Clin Psychopharmacol* 1993, **7**:123-32.
55. JD Amsterdam, J Shults: **MAOI efficacy and safety in advanced stage treatment-resistant depression--a retrospective study.** *J Affect Disord* 2005, **89**:183-8.
56. JW Tiller, P Mitchell, GD Burrows: **Monoamine oxidase inhibitors (MAOI) or reversible inhibitors of monoamine oxidase (RIMA)/tricyclic antidepressant (TCA) combination therapy.** *Aust N Z J Psychiatry* 1992, **26**:327-9.
57. RL Ownby, E Crocco, A Acevedo, V John, D Loewenstein: **Depression and risk for Alzheimer disease - Systematic review, meta-analysis, and metaregression analysis.** *Archives of General Psychiatry* 2006, **63**:530-538.
58. EM Ebly, IM Parhad, DB Hogan, TS Fung: **Prevalence and types of dementia in the very old: results from the Canadian Study of Health and Aging.** *Neurology* 1994, **44**:1593-600.
59. M Goedert, MG Spillantini: **A century of Alzheimer's disease.** *Science* 2006, **314**:777-81.
60. DJ Selkoe: **Alzheimer's disease: genes, proteins, and therapy.** *Physiol Rev* 2001, **81**:741-66.

61. L Bertram, RE Tanzi: **Thirty years of Alzheimer's disease genetics: the implications of systematic meta-analyses.** *Nat Rev Neurosci* 2008, **9**:768-78.
62. DJ Selkoe: **The molecular pathology of Alzheimer's disease.** *Neuron* 1991, **6**:487-98.
63. C Priller, T Bauer, G Mitteregger, B Krebs, HA Kretzschmar, J Herms: **Synapse formation and function is modulated by the amyloid precursor protein.** *J Neurosci* 2006, **26**:7212-21.
64. TL Young-Pearse, J Bai, R Chang, JB Zheng, JJ LoTurco, DJ Selkoe: **A critical function for beta-amyloid precursor protein in neuronal migration revealed by in utero RNA interference.** *J Neurosci* 2007, **27**:14459-69.
65. JS Verbeek, WL Hazenbos, PJ Capel, JG van de Winkel: **The role of FcR in immunity: lessons from gene targeting in mice.** *Res Immunol* 1997, **148**:466-74.
66. J Nunan, DH Small: **Regulation of APP cleavage by alpha-, beta- and gamma-secretases.** *FEBS Lett* 2000, **483**:6-10.
67. MS Wolfe: **The gamma-secretase complex: membrane-embedded proteolytic ensemble.** *Biochemistry* 2006, **45**:7931-9.
68. AE Roher, JD Lowenson, S Clarke, AS Woods, RJ Cotter, E Gowing, MJ Ball: **beta-Amyloid-(1-42) is a major component of cerebrovascular amyloid deposits: implications for the pathology of Alzheimer disease.** *Proc Natl Acad Sci U S A* 1993, **90**:10836-40.
69. MS Brown, J Ye, RB Rawson, JL Goldstein: **Regulated intramembrane proteolysis: a control mechanism conserved from bacteria to humans.** *Cell* 2000, **100**:391-8.
70. WT Kimberly, MJ LaVoie, BL Ostaszewski, WJ Ye, MS Wolfe, DJ Selkoe: **gamma-secretase is a membrane protein complex comprised of presenilin, nicastrin, aph-1, and pen-2.** *Proceedings of the National Academy of Sciences of the United States of America* 2003, **100**:6382-6387.
71. N Gaiano, G Fishell: **The role of Notch in promoting glial and neural stem cell fates.** *Annual Review of Neuroscience* 2002, **25**:471-490.



72. M Baron: **An overview of the Notch signalling pathway.** *Semin Cell Dev Biol* 2003, **14**:113-9.
73. WT Kimberly, MJ LaVoie, BL Ostaszewski, W Ye, MS Wolfe, DJ Selkoe: **Gamma-secretase is a membrane protein complex comprised of presenilin, nicastrin, Aph-1, and Pen-2.** *Proc Natl Acad Sci U S A* 2003, **100**:6382-7.
74. YM Li: **Gamma-secretase: a catalyst of Alzheimer disease and signal transduction.** *Mol Interv* 2001, **1**:198-207.
75. G Thinakaran, DR Borchelt, MK Lee, HH Slunt, L Spitzer, G Kim, T Ratovitsky, F Davenport, C Nordstedt, M Seeger, et al: **Endoproteolysis of presenilin 1 and accumulation of processed derivatives in vivo.** *Neuron* 1996, **17**:181-90.
76. B De Strooper, P Saftig, K Craessaerts, H Vanderstichele, G Guhde, W Annaert, K Von Figura, F Van Leuven: **Deficiency of presenilin-1 inhibits the normal cleavage of amyloid precursor protein.** *Nature* 1998, **391**:387-90.
77. MS Wolfe, W Xia, BL Ostaszewski, TS Diehl, WT Kimberly, DJ Selkoe: **Two transmembrane aspartates in presenilin-1 required for presenilin endoproteolysis and gamma-secretase activity.** *Nature* 1999, **398**:513-7.
78. S Shah, SF Lee, K Tabuchi, YH Hao, C Yu, Q LaPlant, H Ball, CE Dann, T Sudhof, G Yu: **Nicastrin functions as a gamma-secretase-substrate receptor.** *Cell* 2005, **122**:435-447.
79. WT Kimberly, MJ LaVoie, BL Ostaszewski, W Ye, MS Wolfe, DJ Selkoe: **Complex N-linked glycosylated nicastrin associates with active gamma-secretase and undergoes tight cellular regulation.** *J Biol Chem* 2002, **277**:35113-7.
80. JG Culvenor, F Maher, G Evin, F Malchiodi-Albedi, R Cappai, JR Underwood, JB Davis, EH Karran, GW Roberts, K Beyreuther, et al: **Alzheimer's disease-associated presenilin 1 in neuronal cells: evidence for localization to the endoplasmic reticulum-Golgi intermediate compartment.** *J Neurosci Res* 1997, **49**:719-31.

81. SH Pasternak, RD Bagshaw, M Guiral, S Zhang, CA Ackerley, BJ Pak, JW Callahan, DJ Mahuran: **Presenilin-1, nicastrin, amyloid precursor protein, and gamma-secretase activity are co-localized in the lysosomal membrane.** *J Biol Chem* 2003, **278**:26687-94.
82. J Walter, A Capell, J Grunberg, B Pesold, A Schindzielorz, R Prior, MB Podlisny, P Fraser, PS Hyslop, DJ Selkoe, et al: **The Alzheimer's disease-associated presenilins are differentially phosphorylated proteins located predominantly within the endoplasmic reticulum.** *Mol Med* 1996, **2**:673-91.
83. WJ Ray, M Yao, J Mumm, EH Schroeter, P Saftig, M Wolfe, DJ Selkoe, R Kopan, AM Goate: **Cell surface presenilin-1 participates in the gamma-secretase-like proteolysis of Notch.** *J Biol Chem* 1999, **274**:36801-7.
84. WG Annaert, L Levesque, K Craessaerts, I Dierinck, G Snellings, D Westaway, PS George-Hyslop, B Cordell, P Fraser, B De Strooper: **Presenilin 1 controls gamma-secretase processing of amyloid precursor protein in pre-golgi compartments of hippocampal neurons.** *J Cell Biol* 1999, **147**:277-94.
85. M Ankarcrona, K Hultenby: **Presenilin-1 is located in rat mitochondria.** *Biochemical and Biophysical Research Communications* 2002, **295**:766-770.
86. E Area-Gomez, AJC de Groof, I Boldogh, TD Bird, GE Gibson, CM Koehler, WH Yu, KE Duff, MP Yaffe, LA Pon, et al: **Presenilins Are Enriched in Endoplasmic Reticulum Membranes Associated with Mitochondria.** *American Journal of Pathology* 2009, **175**:1810-1816.
87. G Csordas, C Renken, P Varnai, L Walter, D Weaver, KF Buttle, T Balla, CA Mannella, G Hajnoczky: **Structural and functional features and significance of the physical linkage between ER and mitochondria.** *Journal of Cell Biology* 2006, **174**:915-921.
88. C Brou, F Logeat, N Gupta, C Bessia, O LeBail, JR Doedens, A Cumano, P Roux, RA Black, A Israel: **A novel proteolytic cleavage involved in Notch signaling: The role of the disintegrin-metalloprotease TACE.** *Molecular Cell* 2000, **5**:207-216.

89. KA Wharton, KM Johansen, T Xu, S Artavanistsakonas: **Nucleotide-Sequence from the Neurogenic Locus Notch Implies a Gene-Product That Shares Homology with Proteins Containing Egf-Like Repeats.** *Cell* 1985, **43**:567-581.
90. M Baron: **An overview of the Notch signalling pathway.** *Seminars in Cell & Developmental Biology* 2003, **14**:113-119.
91. EC Lai: **Notch signaling: control of cell communication and cell fate.** *Development* 2004, **131**:965-973.
92. A Goate, MC Chartier-Harlin, M Mullan, J Brown, F Crawford, L Fidani, L Giuffra, A Haynes, N Irving, L James, et al: **Segregation of a missense mutation in the amyloid precursor protein gene with familial Alzheimer's disease.** *Nature* 1991, **349**:704-6.
93. EI Rogaeve, R Sherrington, EA Rogaeve, G Levesque, M Ikeda, Y Liang, H Chi, C Lin, K Holman, T Tsuda, et al: **Familial Alzheimer's disease in kindreds with missense mutations in a gene on chromosome 1 related to the Alzheimer's disease type 3 gene.** *Nature* 1995, **376**:775-8.
94. R Sherrington, EI Rogaeve, Y Liang, EA Rogaeve, G Levesque, M Ikeda, H Chi, C Lin, G Li, K Holman, et al: **Cloning of a gene bearing missense mutations in early-onset familial Alzheimer's disease.** *Nature* 1995, **375**:754-60.
95. DR Dries, G Yu: **Assembly, maturation, and trafficking of the gamma-secretase complex in Alzheimer's disease.** *Current Alzheimer Research* 2008, **5**:132-146.
96. J PerezTur, R Croxton, K Wright, H Phillips, C Zehr, R Crook, M Hutton, J Hardy, E Karran, GW Roberts, et al: **A further presenilin 1 mutation in the exon 8 cluster in familial Alzheimer's disease.** *Neurodegeneration* 1996, **5**:207-212.
97. AL Brunkan, AM Goate: **Presenilin function and gamma-secretase activity.** *Journal of Neurochemistry* 2005, **93**:769-792.
98. MJ Smith, JBJ Kwok, CA McLean, JJ Kril, GA Broe, GA Nicholson, R Cappai, M Hallupp, RGH Cotton, CL Masters, et al: **Variable phenotype of Alzheimer's disease with spastic paraparesis.** *Annals of Neurology* 2001, **49**:125-129.

99. ASR Sierksma, DLA van den Hove, HWM Steinbusch, J Prickaerts: **Major depression, cognitive dysfunction and Alzheimer's disease: Is there a link?** *European Journal of Pharmacology* 2010, **626**:72-82.
100. SE Starkstein, R Mizrahi: **Depression in Alzheimer's disease.** *Expert Rev Neurother* 2006, **6**:887-95.
101. T Iwatsubo, A Odaka, N Suzuki, H Mizusawa, N Nukina, Y Ihara: **Visualization of A beta 42(43) and A beta 40 in senile plaques with end-specific A beta monoclonals: evidence that an initially deposited species is A beta 42(43).** *Neuron* 1994, **13**:45-53.
102. C Haass, B De Strooper: **The presenilins in Alzheimer's disease-- proteolysis holds the key.** *Science* 1999, **286**:916-9.
103. AJ Larner, M Doran: **Clinical phenotypic heterogeneity of Alzheimer's disease associated with mutations of the presenilin-1 gene.** *Journal of Neurology* 2006, **253**:139-158.
104. CS Hatchett, S Tyler, D Armstrong, D Dawbarn, SJ Allen: **Familial Alzheimer's disease presenilin 1 mutation M146V increases gamma secretase cutting of p75NTR in vitro.** *Brain Research* 2007, **1147**:248-255.
105. Q Guo, WM Fu, BL Sopher, MW Miller, CB Ware, GM Martin, MP Mattson: **Increased vulnerability of hippocampal neurons to excitotoxic necrosis in presenilin-1 mutant knock-in mice.** *Nature Medicine* 1999, **5**:101-106.
106. MA Leissring, Y Akbari, CM Fanger, MD Cahalan, MP Mattson, FM LaFerla: **Capacitative calcium entry deficits and elevated luminal calcium content in mutant presenilin-1 knockin mice.** *Journal of Cell Biology* 2000, **149**:793-797.
107. IF Smith, B Hitt, KN Green, S Oddo, FM LaFerla: **Enhanced caffeine-induced Ca<sup>2+</sup> release in the 3xTg-AD mouse model of Alzheimer's disease.** *Journal of Neurochemistry* 2005, **94**:1711-1718.
108. SJ Pollack, H Lewis: **Secretase inhibitors for Alzheimer's disease: challenges of a promiscuous protease.** *Curr Opin Investig Drugs* 2005, **6**:35-47.

109. GT Wong, D Manfra, FM Poulet, Q Zhang, H Josien, T Bara, L Engstrom, M Pinzon-Ortiz, JS Fine, HJ Lee, et al: **Chronic treatment with the gamma-secretase inhibitor LY-411,575 inhibits beta-amyloid peptide production and alters lymphopoiesis and intestinal cell differentiation.** *J Biol Chem* 2004, **279**:12876-82.
110. F Panza, V Frisardi, BP Imbimbo, C Capurso, G Logroscino, D Sancarlo, D Seripa, G Vendemiale, A Pilotto, V Solfrizzi: **gamma-Secretase Inhibitors for the Treatment of Alzheimer's Disease: The Current State.** *CNS Neurosci Ther* 2010.
111. HF Dovey, V John, JP Anderson, LZ Chen, P de Saint Andrieu, LY Fang, SB Freedman, B Folmer, E Goldbach, EJ Holsztyńska, et al: **Functional gamma-secretase inhibitors reduce beta-amyloid peptide levels in brain.** *J Neurochem* 2001, **76**:173-81.
112. TA Lanz, CS Himes, G Pallante, L Adams, S Yamazaki, B Amore, KM Merchant: **The gamma-secretase inhibitor N-[N-(3,5-difluorophenacetyl)-L-alanyl]-S-phenylglycine t-butyl ester reduces A beta levels in vivo in plasma and cerebrospinal fluid in young (plaque-free) and aged (plaque-bearing) Tg2576 mice.** *Journal of Pharmacology and Experimental Therapeutics* 2003, **305**:864-71.
113. TA Comery, RL Martone, S Aschmies, KP Atchison, G Diamantidis, X Gong, H Zhou, AF Kreft, MN Pangalos, J Sonnenberg-Reines, et al: **Acute gamma-secretase inhibition improves contextual fear conditioning in the Tg2576 mouse model of Alzheimer's disease.** *J Neurosci* 2005, **25**:8898-902.
114. ER Siemers, JF Quinn, J Kaye, MR Farlow, A Porsteinsson, P Tariot, P Zoulnouni, JE Galvin, DM Holtzman, DS Knopman, et al: **Effects of a gamma-secretase inhibitor in a randomized study of patients with Alzheimer disease.** *Neurology* 2006, **66**:602-4.
115. J Hardy, DJ Selkoe: **The amyloid hypothesis of Alzheimer's disease: progress and problems on the road to therapeutics.** *Science* 2002, **297**:353-6.

116. V Chan-Palay, M Hochli, E Savaskan, G Hungerecker: **Calbindin D-28k and monoamine oxidase A immunoreactive neurons in the nucleus basalis of Meynert in senile dementia of the Alzheimer type and Parkinson's disease.** *Dementia* 1993, **4**:1-15.
117. RL Neve: **Alzheimer's disease sends the wrong signals - a perspective.** *Amyloid-Journal of Protein Folding Disorders* 2008, **15**:1-4.
118. AJ Nazarali, GP Reynolds: **Monoamine neurotransmitters and their metabolites in brain regions in Alzheimer's disease: a postmortem study.** *Cell Mol Neurobiol* 1992, **12**:581-7.
119. L Thorpe, B Groulx: **Depressive syndromes in dementia.** *Can J Neurol Sci* 2001, **28 Suppl 1**:S83-95.
120. L Emilsson, P Saetre, J Balciuniene, A Castensson, N Cairns, EE Jazin: **Increased monoamine oxidase messenger RNA expression levels in frontal cortex of Alzheimer's disease patients.** *Neuroscience Letters* 2002, **326**:56-60.
121. BP Kennedy, MG Ziegler, M Alford, LA Hansen, LJ Thal, E Masliah: **Early and persistent alterations in prefrontal cortex MAO A and B in Alzheimer's disease.** *J Neural Transm* 2003, **110**:789-801.
122. AL Nishimura, C Guindalini, JR Oliveira, R Nitrini, VS Bahia, PR de Brito-Marques, PA Otto, M Zatz: **Monoamine oxidase a polymorphism in Brazilian patients: risk factor for late-onset Alzheimer's disease?** *J Mol Neurosci* 2005, **27**:213-7.
123. M Takehashi, S Tanaka, E Masliah, K Ueda: **Association of monoamine oxidase A gene polymorphism with Alzheimer's disease and Lewy body variant.** *Neuroscience Letters* 2002, **327**:79-82.
124. YH Wu, DF Fischer, DF Swaab: **A promoter polymorphism in the monoamine oxidase A gene is associated with the pineal MAOA activity in Alzheimer's disease patients.** *Brain Res* 2007, **1167**:13-9.
125. R Wang, B Wang, W He, H Zheng: **Wild-type presenilin 1 protects against Alzheimer disease mutation-induced amyloid pathology.** *J Biol Chem* 2006, **281**:15330-6.

126. ND Mehta, LM Refolo, C Eckman, S Sanders, D Yager, J Perez-Tur, S Younkin, K Duff, J Hardy, M Hutton: **Increased Abeta42(43) from cell lines expressing presenilin 1 mutations.** *Annals of Neurology* 1998, **43**:256-8.
127. GA Lyles, BA Callingham: **In vitro and in vivo inhibition by benserazide of clorgyline-resistant amine oxidases in rat cardiovascular tissues.** *Biochem Pharmacol* 1982, **31**:1417-24.
128. X Cao, XM Li, DD Mousseau: **Calcium alters monoamine oxidase-A parameters in human cerebellar and rat glial C6 cell extracts: possible influence by distinct signalling pathways.** *Life Sci* 2009, **85**:262-8.
129. X Cao, Z Wei, GG Gabriel, X Li, DD Mousseau: **Calcium-sensitive regulation of monoamine oxidase-A contributes to the production of peroxyradicals in hippocampal cultures: implications for Alzheimer disease-related pathology.** *BMC Neurosci* 2007, **8**:73.
130. DD Mousseau, AJ Greenshaw: **Chronic effects of clomipramine and clorgyline on regional levels of brain amines and acid metabolites in rats.** *J Neural Transm* 1989, **75**:73-9.
131. RD Porsolt, G Anton, N Blavet, M Jalfre: **Behavioural despair in rats: a new model sensitive to antidepressant treatments.** *European Journal of Pharmacology* 1978, **47**:379-91.
132. DM Nielsen, GJ Carey, LH Gold: **Antidepressant-like activity of corticotropin-releasing factor type-1 receptor antagonists in mice.** *European Journal of Pharmacology* 2004, **499**:135-46.
133. N Kitanaka, J Kitanaka, M Takemura: **Inhibition of methamphetamine-induced hyperlocomotion in mice by clorgyline, a monoamine oxidase-a inhibitor, through alteration of the 5-hydroxytryptamine turnover in the striatum.** *Neuroscience* 2005, **130**:295-308.
134. GG Gabriel: **Characterization of a novel interaction between Presenilin-1 and monoamine oxidase-A.** *University of Saskatchewan M.Sc. Thesis* 2008.
135. CA Hansson, S Frykman, MR Farmery, LO Tjernberg, C Nilsberth, SE Pursglove, A Ito, B Winblad, RF Cowburn, J Thyberg, et al: **Nicastrin,**

- presenilin, APH-1, and PEN-2 form active gamma-secretase complexes in mitochondria.** *J Biol Chem* 2004, **279**:51654-60.
136. E Area-Gomez, AJ de Groof, I Boldogh, TD Bird, GE Gibson, CM Koehler, WH Yu, KE Duff, MP Yaffe, LA Pon, et al: **Presenilins are enriched in endoplasmic reticulum membranes associated with mitochondria.** *American Journal of Pathology* 2009, **175**:1810-6.
137. N Wiedemann, C Meisinger, N Pfanner: **Cell biology. Connecting organelles.** *Science* 2009, **325**:403-4.
138. DG Jo, JW Chang, HS Hong, I Mook-Jung, YK Jung: **Contribution of presenilin/gamma-secretase to calsenilin-mediated apoptosis.** *Biochem Biophys Res Commun* 2003, **305**:62-6.
139. Y Morohashi, T Kan, Y Tominari, H Fuwa, Y Okamura, N Watanabe, C Sato, H Natsugari, T Fukuyama, T Iwatsubo, et al: **C-terminal fragment of presenilin is the molecular target of a dipeptidic gamma-secretase-specific inhibitor DAPT (N-[N-(3,5-difluorophenacetyl)-L-alanyl]-S-phenylglycine t-butyl ester).** *J Biol Chem* 2006, **281**:14670-6.
140. ME Szapacs, AL Numis, AM Andrews: **Late onset loss of hippocampal 5-HT and NE is accompanied by increases in BDNF protein expression in mice co-expressing mutant APP and PS1.** *Neurobiology of Disease* 2004, **16**:572-580.
141. Y Liu, MJ Yoo, A Savonenko, W Stirling, DL Price, DR Borchelt, L Mamounas, WE Lyons, ME Blue, MK Lee: **Amyloid pathology is associated with progressive monoaminergic neurodegeneration in a transgenic mouse model of Alzheimer's disease.** *J Neurosci* 2008, **28**:13805-14.
142. AS Yoo, I Cheng, S Chung, TZ Grenfell, H Lee, E Pack-Chung, M Handler, J Shen, W Xia, G Tesco, et al: **Presenilin-mediated modulation of capacitative calcium entry.** *Neuron* 2000, **27**:561-72.
143. Q Guo, K Furukawa, BL Sopher, DG Pham, J Xie, N Robinson, GM Martin, MP Mattson: **Alzheimer's PS-1 mutation perturbs calcium homeostasis and sensitizes PC12 cells to death induced by amyloid beta-peptide.** *Neuroreport* 1996, **8**:379-83.



144. I Schneider, D Reverse, I Dewachter, L Ris, N Caluwaerts, C Kuiperi, M Gilis, H Geerts, H Kretzschmar, E Godaux, et al: **Mutant presenilins disturb neuronal calcium homeostasis in the brain of transgenic mice, decreasing the threshold for excitotoxicity and facilitating long-term potentiation.** *Journal of Biological Chemistry* 2001, **276**:11539-11544.
145. DL Price, SS Sisodia: **Mutant genes in familial Alzheimer's disease and transgenic models.** *Annu Rev Neurosci* 1998, **21**:479-505.
146. J Shen, RT Bronson, DF Chen, W Xia, DJ Selkoe, S Tonegawa: **Skeletal and CNS defects in Presenilin-1-deficient mice.** *Cell* 1997, **89**:629-39.
147. M Wines-Samuelson, M Handler, J Shen: **Role of presenilin-1 in cortical lamination and survival of Cajal-Retzius neurons.** *Dev Biol* 2005, **277**:332-46.
148. A Louvi, SS Sisodia, EA Grove: **Presenilin 1 in migration and morphogenesis in the central nervous system.** *Development* 2004, **131**:3093-105.
149. O Cases, T Vitalis, I Seif, E De Maeyer, C Sotelo, P Gaspar: **Lack of barrels in the somatosensory cortex of monoamine oxidase A-deficient mice: role of a serotonin excess during the critical period.** *Neuron* 1996, **16**:297-307.
150. B Petit-Demouliere, F Chenu, M Bourin: **Forced swimming test in mice: a review of antidepressant activity.** *Psychopharmacology (Berl)* 2005, **177**:245-55.
151. K Ritchie, S Lovestone: **The dementias.** *Lancet* 2002, **360**:1759-66.
152. NA Garrick, M Scheinin, WH Chang, M Linnoila, DL Murphy: **Differential effects of clorgyline on catecholamine and indoleamine metabolites in the cerebrospinal fluid of rhesus monkeys.** *Biochem Pharmacol* 1984, **33**:1423-7.
153. Y Kitaichi, T Inoue, S Nakagawa, T Izumi, T Koyama: **Effect of co-administration of subchronic lithium pretreatment and acute MAO inhibitors on extracellular monoamine levels and the expression of contextual conditioned fear in rats.** *Eur J Pharmacol* 2006, **532**:236-45.

154. M Prieto, MT Giralt: **Desensitization of alpha(2)-adrenoceptors which regulate noradrenaline synthesis and release after chronic treatment with clorgyline in the rat brain.** *Pharmacology* 2002, **65**:49-56.
155. O Berezovska, A Lleo, LD Herl, MP Frosch, EA Stern, BJ Bacskai, BT Hyman: **Familial Alzheimer's disease presenilin 1 mutations cause alterations in the conformation of presenilin and interactions with amyloid precursor protein.** *J Neurosci* 2005, **25**:3009-17.
156. DE Kang, IS Yoon, E Repetto, T Busse, N Yermian, L Ie, EH Koo: **Presenilins mediate phosphatidylinositol 3-kinase/AKT and ERK activation via select signaling receptors. Selectivity of PS2 in platelet-derived growth factor signaling.** *J Biol Chem* 2005, **280**:31537-47.

## APPENDIX



Lewei Rui <lewei.rui@gmail.com>

---

### requesting permission to use one figure in my M.Sc.thesis

2 messages

---

Lewei Rui <lewei.rui@gmail.com>  
To: PNASPermissions@nas.edu

Wed, Nov 17, 2010 at 1:42 PM

To whom it may concern,

My name is Lewei Rui. I am a M.Sc. student at Department of Psychiatry, University of Saskatchewan, Canada. I would like to use Fig.2 titled "The overall structure of hMAO-A (A)" from the article

"Three-Dimensional Structure of Human Monoamine Oxidase A (MAO A): Relation to the Structures of Rat MAOA and Human MAO-B". ProNatl Acad Sci U S A 102(36): 12684-12689

as part of my M.Sc. thesis titled "Interaction between PS-1 and MAO-A: implication of the relation between Alzheimer's disease and Depression". I would be so appreciate if you could grant me permission to use this one figure only for my thesis paper. Thank you so much for your consideration.

Sincerely,

Lewei Rui

Department of Psychiatry  
University of Saskatchewan  
[lewei.rui@gmail.com](mailto:lewei.rui@gmail.com)

---

PNAS Permissions <PNASPermissions@nas.edu>  
To: Lewei Rui <lewei.rui@gmail.com>

Mon, Nov 29, 2010 at 11:32 AM

Dear Lewei Rui,

Permission is granted for your use of the figure as described in your message below. Please cite the full journal references and "Copyright (copyright year) National Academy of Sciences, U.S.A."

Please let us know if you have any questions!

Best regards,

Kat Rodenhizer for

Diane Sullenberger

<https://mail.google.com/mail/?ui=2&ik=b33dfa5253&view=pt&search=Inbox&th=12c5b5c24b3288be>

Page 1 of 2

Executive Editor

PNAS

---

**From:** Lewei Rui [mailto:[lewei\\_rui@gmail.com](mailto:lewei_rui@gmail.com)]  
**Sent:** Wednesday, November 17, 2010 2:43 PM  
**To:** PNAS Permissions  
**Subject:** requesting permission to use one figure in my M.Sc.thesis

[Quoted text hidden]

---



Permissions Letter

Ref# 11-30123

DATE: Friday, January 21, 2011

TO: Lewei Rui  
Department of Psychiatry  
University of Saskatchewan  
B46 Health Sciences Bldg.  
107 Wiggins Road  
Saskatoon, SK S7N 5E5 Canada

FROM: Elizabeth Sandler, Rights and Permissions  
RE: Your request for permission dated 01/03/11

Permission is valid for use of the following AAAS material only:

Fig 2 from Hardy & Selkoe, SCIENCE 297:353 (2002)

In the following work only:

M.SC. THESIS

FEE: Permission fees are waived in this instance. AAAS reserves the right to charge for reproduction of AAAS controlled material in the future.

Regarding your request, we are pleased to grant you non-exclusive, non-transferable permission, to republish the AAAS material identified above in your work identified above, subject to the terms and conditions herein. We must be contacted for permission for any uses other than those specifically identified in your request above.

The following credit line must be printed along with the AAAS material: "From [Full Reference Citation]. Reprinted with permission from AAAS."

All required credit lines and notices must be visible any time a user accesses any part of the AAAS material and must appear on any printed copies and authorized user might make.

This permission does not apply to figures / photos / artwork or any other content or materials included in your work that are credited to non-AAAS sources. If the requested material is sourced to or references non-AAAS sources, you must obtain authorization from that source as well before using that material. You agree to hold harmless and indemnify AAAS against any claims arising from your use of any content in your work that is credited to non-AAAS sources.

If the AAAS material covered by this permission was published in Science during the years 1974 - 1994, you must also obtain permission from the author, who may grant or withhold permission, and who may or may not charge a fee if permission is granted. See original article for author's address. This condition does not apply to news articles.

The AAAS material may not be modified or altered except that figures and tables may be modified with permission from the author. Author permission for any such changes must be secured prior to your use.

Whenever possible, we ask that electronic uses of the AAAS material permitted herein include a hyperlink to the original work on AAAS's website (hyperlink may be embedded in the reference citation).

AAAS material reproduced in your work identified herein must not account for more than 30% of the total contents of that work.

AAAS must publish the full paper prior to use of any text.

*Headquarters:  
1200 New York Avenue, NW, Washington, D.C. 20005 USA*

AAAS material must not imply any endorsement by the American Association for the Advancement of Science.

This permission is not valid for the use of the AAAS and/or Science logos.

AAAS makes no representations or warranties as to the accuracy of any information contained in the AAAS material covered by this permission, including any warranties of merchantability or fitness for a particular purpose.

If permission fees for this use are waived, please note that AAAS reserves the right to charge for reproduction of this material in the future.

Permission is not valid unless payment is received within sixty (60) days of the issuance of this permission. If payment is not received within this time period then all rights granted herein shall be revoked and this permission will be considered null and void.

This Permission may not be amended except by written document signed by both parties. The terms above are applicable to all permissions granted for the use of AAAS material. Below you will find additional conditions that apply to your particular type of use.

**FOR A THESIS OR DISSERTATION**

If you are using figure(s)/table(s), permission is granted for use in print and electronic versions of your dissertation or thesis. A full text article may be used in print versions only of a dissertation or thesis.

Permission covers the distribution of your dissertation or thesis on demand by ProQuest / UMI, provided the AAAS material covered by this permission remains in situ.

If you are an Original Author on the AAAS article being reproduced, please refer to your License to Publish for rules on reproducing your paper in a dissertation or thesis.

---

By using the AAAS Material identified in your request, you agree to abide by all the terms and conditions herein.

Questions about these terms can be directed to the AAAS Permissions department [permissions@aaas.org](mailto:permissions@aaas.org).

*Headquarters:  
1200 New York Avenue, NW, Washington, D.C. 20005 USA*



*Council*

**James R. Halpert**  
*President*  
University of California, San Diego

**Brian M. Cox**  
*Past President*  
Uniformed Services University  
of the Health Sciences

**Lynn Wecker**  
*President-Elect*  
University of South Florida

**Bryan F. Cox**  
*Secretary/Treasurer*  
Abbott Laboratories

**David R. Sibley**  
*Past Secretary/Treasurer*  
National Institute of Neurological  
Disorders and Stroke

**Mary E. Vore**  
*Secretary/Treasurer-Elect*  
University of Kentucky

**Stephen M. Lanier**  
*Councilor*  
Medical University of South Carolina

**Suzanne G. Laychock**  
*Councilor*  
State University of New York at Buffalo

**Richard R. Neubig**  
*Councilor*  
University of Michigan

**James E. Barrett**  
*Board of Publications Trustee*  
*FASEB Board Representative*  
Drexel University

**Jack Bergman**  
*Program Committee*  
Harvard Medical School - McLean  
Hospital

**Christine K. Carrico**  
*Executive Officer*

9650 Rockville Pike  
Bethesda, MD 20814-3995

Phone: (301) 634-7060  
Fax: (301) 634-7061

info@aspet.org  
www.aspet.org

November 19, 2010

Lewei Rui  
Psychiatry  
107 Wiggins Road  
Saskatoon, Saskatchewan S7N 5E5  
Canada

Email: lewei.rui@usask.ca

Dear Lewei Rui:

This is to grant you permission to reproduce the following figure in your thesis titled, "Interaction of PS-1 and MAO-A: Implication of the Relation between Alzheimer's Disease and Depression" for the University of Saskatchewan:

Figure 2 from Yue-Ming Li,  $\gamma$ -Secretase: A Catalyst of Alzheimer Disease and Signal Transduction, *Mol Interv* October 2001 1:198-207

Permission to reproduce the figure is granted for worldwide use in all languages, translations, and editions, and in any format or medium including print and electronic. The authors and the source of the materials must be cited in full, including the article title, journal title, volume, year, and page numbers.

Sincerely yours,

Richard Dodenhoff  
Journals Director

**American Society for Pharmacology and Experimental Therapeutics**